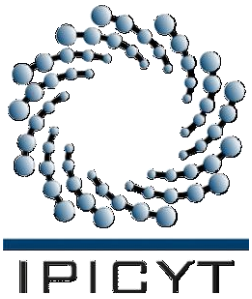

INSTITUTO POTOSINO DE INVESTIGACIÓN CIENTÍFICA Y TECNOLÓGICA, A.C.

POSGRADO EN CIENCIAS EN BIOLOGÍA MOLECULAR

"IPI-SA3-C4, population of human preadipose cells with multipotent differentiation capability. Characterization as a model system for *in vitro* adipogenesis and optimization of its culture conditions**"**

Tesis que presenta

Claudia Griselda Cárdenas León

Para obtener el grado de

Doctora en Ciencias en Biología Molecular

Director de tesis

Dr. Luis Antonio Salazar Olivo

San Luis Potosí, S.L.P., Julio de 2020

Constancia de aprobación de la tesis

La tesis “IPI-SA3-C4, population of human preadipose cells with multipotent differentiation capability. Characterization as a model system for *in vitro* adipogenesis and optimization of its culture conditions” presentada para obtener el Grado de Doctora en Ciencias en Biología Molecular fue elaborada por **Claudia Griselda Cárdenas León** y aprobada el **16 de Julio de 2020** por los suscritos, designados por el Colegio de Profesores de la División de Biología Molecular del Instituto Potosino de Investigación Científica y Tecnológica, A.C.

_____
Dr. Luis Antonio Salazar Olivo
Director de la tesis

_____
Dr. Federico Castro Muñozledo
Asesor

_____
Dr. Antonio De León Rodríguez
Asesor

_____
Dra. Gerardo Argüello Astorga
Asesor

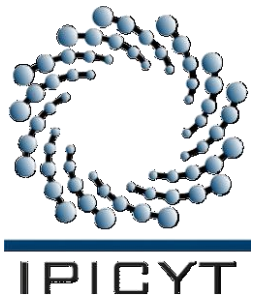

Créditos institucionales

Esta tesis se desarrolló en dos instituciones: el Laboratorio de Biotecnología Médica y Pecuaria de la División de Biología Molecular del Instituto Potosino de Investigación Científica y Tecnológica, A.C., bajo la dirección del Dr. Luis Antonio Salazar Olivo, y en el Grupo de Células Troncales Somáticas y Regeneración de la Universidad de Tartu, Estonia, bajo la supervisión del Dr. Viljar Jaks y la dirección del Dr. Luis Antonio Salazar Olivo. Dos publicaciones se generaron para sostener el título de Doctor en ciencias en Biología Molecular.

Durante la realización del trabajo la autora recibió una beca académica del Consejo Nacional de Ciencia y Tecnología (número de registro 330683) y la beca Dora Plus sub-actividad 2.2 financiada por el Fondo Europeo de Desarrollo Regional Europea y la República de Estonia.

Instituto Potosino de Investigación Científica y Tecnológica, A.C.

Acta de Examen de Grado

El Secretario Académico del Instituto Potosino de Investigación Científica y Tecnológica, A.C., certifica que en el Acta 111 del Libro Segundo de Actas de Exámenes de Grado del Programa de Doctorado en Ciencias en Biología Molecular está asentado lo siguiente:

En la ciudad de San Luis Potosí a los 16 días del mes de julio del año 2020, se reunió a las 12:00 horas en las instalaciones del Instituto Potosino de Investigación Científica y Tecnológica, A.C., el Jurado integrado por:

Dr. Antonio De León Rodríguez	**Presidente**	**IPICYT**
Dr. Luis Antonio Salazar Olivo	**Secretario**	**IPICYT**
Dr. Gerardo Rafael Argüello Astorga	**Sinodal**	**IPICYT**
Dr. Rubén Hipólito López Revilla	**Sinodal**	**IPICYT**

a fin de efectuar el examen, que para obtener el Grado de:

DOCTORA EN CIENCIAS EN BIOLOGÍA MOLECULAR

sustentó la C.

Claudia Griselda Cárdenas León

sobre la Tesis intitulada:

IPI-SA3-C4, population of human preadipose cells with multipotent differentiation capability. Characterization as a model system for in vitro adipogenesis and optimization of its culture conditions

que se desarrolló bajo la dirección de

Dr. Luis Antonio Salazar Olivo

El Jurado, después de deliberar, determinó

APROBARLA

Dándose por terminado el acto a las 14:22 horas, procediendo a la firma del Acta los integrantes del Jurado. Dando fe el Secretario Académico del Instituto.

A petición de la interesada y para los fines que a la misma convengan, se extiende el presente documento en la ciudad de San Luis Potosí, S.L.P., México, a los 16 días del mes de julio de 2020.

Dr. Marcial Bonilla Marín
Secretario Académico

Mtra. Ivonne Lizette Cuevas Vélez
Jefa del Departamento del Posgrado

INSTITUTO POTOSINO DE INVESTIGACIÓN CIENTÍFICA Y TECNOLÓGICA, A.C.
IPICYT
SECRETARIA ACADEMICA

Dedications

A mi familia, que me llena de energía para seguir adelante.

To the people that I met in all this long journey, at each one I have in the memory.

Viljar ja Imbi Jaks, te hoidsite mind palju, pole piisavalt sõnu, et tänada.

Vahtra pere, te andsite mulle nii palju rõõmu, seiklusi, tuge ja armastust, suured tänud teile.

Thanks

To CONACYT for the graduate fellowship no. 330683 and to Republic of Estonia for the scholarship Dora Plus sub-Action 2.2 from European Regional Development Fund.

To Instituto Potosino e Investigación Científica y Tecnológica, México, and Tartu University, Estonia, for allow me to develop my experimental work.

To Dr. Luis Salazar Olivo and Dr. Viljar Jaks for guiding me, support me and be patient with me.

To Dr. Federico Castro Muñozledo, Dr. Antonio De León Rodríguez, and Dr. Gerardo Rafael Argüello Astorga for their comments and constant review of documents.

To Dr. Angélica Montoya Contreras and Biol. Mireya Guadalupe Sánchez Garza for the technical and academic support provided for the development of this work in Mexico.

To Dr. Kristina Mäemets Allas, Dr. Mariliis Klaas, Dmitri Lubenets, and Kati Kuuse for the technical and academic support provided for the development of this work in Estonia.

Content

Abbreviations

2-NBDG	2-[N-(7-nitrobenz-2-oxa-1,3-diazol-4-yl)amino]-2-deoxy-D-glucose
3T3	Mouse Swiss embryonic fibroblast cell line obtained by serial subculture
BIBR	Synthetic, non-nucleosidic compound, telomerase inhibitor BIBR1532
C/EBP	CCAAT/enhancer-binding proteins
CD	Cluster of differentiation
Chub-S7	Stromal cells derived from human adipose tissue immortalized with hTERT y E7
CRISPR	Clustered regularly interspaced short palindromic repeats
DAPI	4',6-diamidino-2-´henylindole
DMSO	Dimethyl sulfoxide
DTT	Dithiothreitol
E6	Oncoprotein *E6* of human papillomavirus type 16
E7	Oncoprotein *E7* of human papillomavirus type 16
EBV	Epstein-Barr virus
EDTA	Ethylenediaminetetraacetic acid
FBS	Fetal bovine serum
GAPDH	Glyceraldehyde 3-phosphate dehydrogenase
GPDH	Glycerol-3- phosphate dehydrogenase
hASC-TE	Human adipose-derived stromal cells immortalized by hTERT, and E6/E7
HCl	Hydrochloric acid
hESC	Human embryonic stem cells
HLA-DR	Human leukocyte antigen DR
hMSC-hTERT-E6/E7	Human mesenchymal stromal cells derived from bone marrow immortalized by hTERT and E6/E7
IPI-SA3-C4	Clone 4 obtained from the third human subcutaneous adipose tissue sample processed at IPICYT
KCl	Potassium chloride
M1	Mortality stage 1 (replicative senescence)
M2	Mortality stage 2 (crisis)
BM	Basal culture medium
AM	Adipogenic culture medium
MM	Maintaining culture medium
MSC	Mesenchymal stromal cells
P16	Tumor suppressor protein 16
P53	Tumor suppressor protein 53
PBS	Phosphate buffered saline
PDTs	Population doubling time
PDLs	Population doublings level
PPARγ	Peroxisome proliferator-activated receptor, gamma
Rb	Retinoblastoma protein
RT	Reverse transcriptase
S/MARs	Scaffold/matrix attachment region

SA-β-Gal	Senescence-asociated-β-galactosidase
SDS	Sodium dodecyl sulfate
SGBS	Simpson-Golabi-Behemil syndrome
SV40gp6	Gene of large T antigen of the simian virus 40
SVF	Stromal vascular fraction
TERT	Enzyme telomerase reverse transcriptase
TGF	Transforming growth factor

IPI-SA3-C4, population of human preadipose cells with multipotent differentiation capability. Characterization as a model system for *in vitro* adipogenesis and optimization of its culture conditions

Abstract

The most commonly *in vitro* model systems used for adipose tissue studies are murine cell lines, which have genetic and metabolic differences with the human adipocytes. To date, there is not a general *in vitro* model to study the human adipose tissue, because adipogenic human cell lines have a low adipogenic potential and their use is limited. This thesis includes two reports: the first one describes the characterization of a human subcutaneous adipose stromal cell population, “IPI-SA3-C4”, while the second one deals with the optimization of the culture medium for growing these cells. The IPI-SA3-C4 population is composed of non-tumorigenic diploid cells with high proliferative potential as well as strong adipogenic, osteogenic and chondrogenic differentiation capabilities. In the second report, we proved that a dilution 1:1 of L15 and mTeSR1 culture media allow to expand the life span of these cells in 20%, while retains their adipogenic capacity and normal diploid karyotype. Thus, this work describes the IPI-SA3-C4 cells as a new *in vitro* model system suitable but transient to study the human adipose tissue as well a cell culture strategy assuring high *in vitro* expansion of normal adult mesenchymal stromal cells useful for basic and translational research.

IPI-SA3-C4, población de células preadiposas humanas con capacidad de diferenciación multilinaje. Caracterización como un sistema modelo para la adipogénesis *in vitro* y optimización de sus condiciones de cultivo.

Resumen

Los modelos *in vitro* más utilizados para el estudio del tejido adiposo son líneas celulares de origen múrido, las cuales presentan diferencias genéticas y metabólicas respecto a los adipocitos humanos. Hasta ahora no hay un modelo *in vitro* de adipogénesis humana de uso generalizado, porque las líneas celulares adiposas humanas descritas habitualmente tienen un bajo potencial adipogénico y su uso es limitado. Este trabajo de tesis resultó en dos reportes: El primero describe la caracterización de una población de células estromales adiposas subcutáneas humanas, "IPI-SA3-C4", en tanto que el segundo trata de la optimización del medio de cultivo para el crecimiento de estas células. La población IPI-SA3-C4 está constituida por células diploides, no tumorigénicas, con alto potencial proliferativo y con una fuerte capacidad de diferenciación adipogénica, osteogénica y condrogénica. En el segundo reporte probamos que una mezcla 1:1 de medios de cultivo L15 y mTeSR1 permiten expandir la esperanza de vida de estas células en un 20%, al tiempo que mantiene su capacidad adipogénica y su cariotipo diploide normal. Así, este trabajo describe las células IPI-SA3-C4 como un modelo *in vitro* adecuado aunque transitorio para estudiar el tejido adiposo humano y una estrategia de cultivo celular que permite la alta expansión *in vitro* de células estromales mesenquimales adultas normales con utilidad para investigación básica y traslacional.

1. Introduction

This thesis work encompasses two parts, the first part includes the characterization of a cellular population *in vitro*, which was derived from a young donor, and which because of its high capacities of proliferation and adipogenic differentiation on preliminary assays, led us to carry out its detailed characterization. While, the second part of the thesis, we developed a novel cell culture strategy that enhances the *in vitro* proliferative capacity of normal mesenchymal stromal cells derived from human adipose tissue.

1.1. Adipose tissue and adipogenesis

Adipose tissue is the main site of energy storage and mobilization in higher eukaryotes. It stores triglycerides in periods of high food availability and mobilize them during food deprivation (González-Casanova et al., 2020). Adipose tissue is classified by its morphological and biochemical characteristics into two basic types: withe adipose tissue (WAT) and brown adipose tissue (BAT), although a third adipose phenotype, the beige or brite adipocytes, can be induced in WAT. WAT also perform endocrine functions since it produces and releases proteins involved in the metabolic regulation, reproduction, immunity and others functions (Chait et al., 2020). For example, leptin, a hormone produced and released by mature WAT adipocytes, acts as a satiety signal by interacting with its hypothalamic receptor, besides participating in regulation of menstrual cycle, and reproductive function (Aragonès et al., 2016; Catteau et al., 2016). Furthermore, WAT is the major component of adipose tissue in mammals (~80%), and its study is essential to

understand the mechanisms involved in dysfunctions that account for a huge burden on the health care system worldwide such as obesity, type 2 diabetes, hypertension and certain types of cancer(González-Casanova et al., 2020).

WAT can be studied *in vivo* by the use of experimental animal models like rats, mice, pigs, and others, but they have differences with humans, besides they have high-cost maintenance. Such limitations have opened the door to use of *in vitro* models. These systems have been derived from fat tissue biopsies and show a heterogeneous composition that permits to find different cellular types, mainly mature adipocytes, but also endothelial cells, fibroblasts, preadipocytes, and mesenchymal stromal cells (Armani et al., 2010). The fibroblasts, preadipocytes, and mesenchymal stromal cells are plastic adherent, they proliferate potentially, but just the preadipocytes, and mesenchymal stromal cells have the capacity to originate new and specialized cellular adipose cells, through a differentiation process called adipogenesis (González-Casanova et al., 2020). Adipogenesis is a gradual process in which small fibroblast-like cells undergo metabolic, morphologic and gene expression changes that culminate in bigger spherical cells that store fat (Ruiz-Ojeda et al., 2016). To evaluate the adipogenic ability of the cells, the next process takes place. First, the cells are grown under specific temperature and humidity conditions in a standard culture medium until they become confluent, or undergo growth arrest. Afterwards, a specific mix of growth factors, and hormonal/chemical inductors termed as “adipogenic cocktail” is added to the standard culture medium by a specific number of days to induce the differentiation into adipocytes. Subsequently, cells are maintained in the standard culture medium

with appropriate growth factors but without inductors (Cristancho et al., 2011; Armani et al., 2010). Generally, the adipogenic cocktail consists of insulin, glucocorticoids, methylisobutylxanthine (MIX), and fetal bovine serum (Armani et al., 2010). During adipogenesis, a sequential cascade of gene expression is involved, wherein the expression of the CCAAT/enhancer binding proteins β and δ (C/EBPβ, C/EBPδ) is required during the initial phase. Thereafter, both proteins induce C/EBPα and proliferator-activated receptor gamma (PPARγ) expression. The last one is considered the master regulator of the adipogenesis, because after its expression, the morphological changes characteristic of adipose conversion are developed and the expression of genes of mature adipocytes is induced, as occurs for fatty acid-binding protein 4, leptin, and others. (González-Casanova et al., 2020).

1.2. Primary cultures, preadipocytes, and mesenchymal stromal cells

The *in vitro* models to study white adipose tissue are primary cultures and established cell lines. Primary cultures are obtained by disaggregation of a fresh tissue piece by mechanical and/or enzymatical treatment. From these, cells might be isolated, usually by its adherence to plastic culture dishes, or by cells sorting using specific surface markers before plating of the cells (Jozefczuk et al., 2012; Church et al., 2014). Moreover, primary cells represent high fidelity the *in vivo* metabolism of the tissue from which they were derived, and their proliferative and differentiation capacities decreases as the cells spend more time in culture (Zuk et al., 2001).

For instance, when the adipose tissue is treated mechanically or enzymatically and separated by centrifugation, it is possible to obtain the stromal vascular fraction (SVF). SVF is a heterogeneous cell population that comprises diverse cell types such as fibroblasts, preadipocytes, leukocytes, epithelial and endothelial cells, as well as others (Cawthorn et al., 2012). However, when the SVF is cultivated just some cells have the ability to adhere and grow, but only the preadipocytes and stem cells will have the ability to undergo differentiation into mature adipocytes. The name “preadipocyte” makes mention to cells present in adipose tissue which are precursors of mature adipocytes (Cawthorn et al., 2012). On the other hand, Mesenchymal Stromal/Stem Cells (MSCs) are other cell type that may develop into a wide variety of tissues, like adipose tissue, dental pulp, bone marrow, extra-embryonic tissues, and others (Heo et al., 2016). These cells possess stemness characteristics as high proliferative capacity and the ability of multilineage differentiation. However, Mesenchymal Stromal Cell Committee of the International Society for Cellular Therapy recently established the minimal criteria to be met to name them as Mesenchymal Stem Cells. Independently of the tissue of origin, MSCs, are plastic adherent cells which express CD37, CD90, and CD105 as positives surface markers, as well as CD11b, CD14, CD19, CD34, CD45, CD79, and HLA-DR negatives (Viswanathan et al., 2019). Moreover, MSCs should have the capacity to differentiate into at least three different lineages: adipocytes, osteoblasts, and chondrocytes, although they could be induced to differentiate into other cell lineages such as myoblasts, neurons, and others (Viswanathan et al., 2019; Guasti et al., 2018).

1.3. Life-span and cellular senescence

In spite of the advantages that primary cultures possess to study a specific tissue, all normal cells are limited life-span; a statistical measure of the average time in which cells can proliferate (Sikora et al., 2018). Hayflick, showed for the first time in 1965 this phenomenon during the *in vitro* cultivation of human fetal diploid cells. He observed that after 50 ± 10 Population Doubling Level (PDL) cells entered in a stable proliferative arrest in which they remained viable for many months, now denominated Hyflick limit (Hayflick, 1965; Bond et al., 1999). Since then, cellular aging has been widely studied *in vitro*; currently, growth arrest is called replicative senescence and constitutes one of the inherent controls for normal cell proliferation. It is also named mortality stage 1 (M1) (Bond et al., 1999), and is characterized by the lack of proliferation in the senescent cells, which remain alive but they are not dividing. During this stage, cells undergo morphological alterations consisting in an enlarged and irregular shape, but also show increased levels of cell cycle inhibitors such as p16 and p51, and increased DNA damage response, and (Sikora et al., 2018). Usually, the entry of cells into M1 occurs after 40 to 70 population doublings, when telomere erosion is achieved, but this phenomenon depends on the age of the donor (Hayflick, 1965; Bond et al., 1999). The telomere erosion is a process that arises from the inactivation of the enzyme telomerase reverse transcriptase (TERT) which is necessary for maintaining telomere length. Thus TERT inactivation triggers the telomere shortening during DNA replication. Because of this, young cells possess long telomeres, show high TERT activity, and proliferate largest periods in cell culture, in contrast with older cells (Bond et al., 1999). If senescent cells survive the M1 stage and continue proliferating, they face

to the second inherent proliferative control of normal cells, called crisis or M2 stage, which is characterized by massive cellular death (Fridman et al., 2008). The rare cells that escape the crisis undergo immortalization, and their telomeres become stabilized by the reactivation of TERT or another equivalent mechanisms (Fridman et al., 2008). However, the accumulation of DNA damage may induce transformation, and cells acquire tumorigenic capacity and show an aberrant chromosomal complement (Sikora et al., 2008).

1.4. Cell lines and immortalization methods

Cell lines are cells with unlimited proliferative capacity that no necessarily possess the functional attributes of the tissue from which they were derived, their origin is the same as that of the primary cultures. However, to obtain a cell line an immortalization process is carried out in which usually the proliferative, and differentiation properties of the cells are changed, as well as the chromosomal complement (Freshney, 2010), but the possible alterations to the original properties depend on the strategy utilized (Conese et al., 2004).

There are diverse immortalization methods, which principally include the spontaneous immortalization by serial subculture (Todaro and Green, 1963), or the overexpression of immortalizing genes (Lo and Yee, 2007). The spontaneous immortalization consists in obtaining primary cultures from normal tissues, afterwards cells are serially subcultured at a specific plating density, and following a specific time between subcultures (Todaro immortalization method; Todaro and Green, 1963). Between the first cell lines produced by this method we find the 3T3,

3T6, and 3T12 cell lines obtained by Todaro and Green in 1963. In such study, the authors showed the effect of plating density, and subculture schedule on the proliferation of mouse embryonic fibroblasts during long-term cultivation *in vitro*, thus they established a spontaneous immortalization method, which is still used to obtain cell lines of mammalian, but rarely for human cells.

To overexpress immortalizing genes, techniques as transduction/transfection are required, where generally cationic lipid, electroporation, calcium phosphate, and CRISPR transfection methods are used but mainly viral particles with sequences of interest are produced to obtain a stable transfection, which requires the DNA integration (Lo and Yee, 2007). The viral particles to produce are generally retrovirus, but also lentivirus, adenovirus, or others. The first two develop a stable integration process, while the third not, they trigger a transient process. Actually, more than one vector requires to be transfected in an easily transfected cell line as HEK293 cells, to produce viruses without reproducibility capacity, which carry out the sequence of interest to overexpress (Lo and Yee, 2007). Where, generally the sequences of interest are integrated into the genome of the cells (integration process), increasing the risk to develop insertional mutagenesis and/or malignization (Conese et al., 2004).

Other tools that can be used to overexpress sequences of interest, such as episomal self-replicating systems, non-integrative vectors, with self-replication capacity and extrachromosomal maintenance, which have a prolonged but transient transgene expression after transfecting the target cells (Conese et al., 2004). For example, vectors derived from the Epstein-Barr virus (EBV) that possess sequences as EBNA1, and oriP, which act together to be replicated and

retained in the nucleus (Conese et al., 2004). Other vectors containing scaffold/matrix attachment region (S/MARs) or artificial chromosomes possess specific sequences that are used to overexpress sequences of interest and maintained as episomal vectors (Conese et al., 2004). However, these systems have been scarcely used to immortalize cells. Moreover, the conditional immortalization process can be developed, where the conditional expression of the sequence of interest at permissible temperature allow control the continuous culture and growth of these cells, but the affectivity is not clear (Church et al., 2014).

To immortalize cells sequences with a viral origin usually are used, for example, *SV40gp6* of the simian virus 40, *E6*, and *E7* of human papillomavirus type 16 (Balducci et al., 2014), which permit to scape of M1 (Bond et al., 1999). Because, the large T antigen of the simian virus 40 inactivate the tumor suppressor protein p53, while the E6 protein accelerates its degradation, also the E7 protein stops the cellular function of retinoblastoma (Rb), other tumor suppressor protein (Drayman et al., 2016; Takeuchi et al., 2007). The p53 and Rb proteins are important regulators of cell cycle and their inactivation carries with the abnormal chromosomal segregation, genetic instability and increases the risk to malignancy (Takeuchi et al., 2007). Other sequences with no viral origin are used to immortalize, these are present in the human genome, but their expression are sometimes low or null, for example, oncogenes as H-RAS, C-MYC (Kelekar and Cole, 1987), TERT (Darimont et al., 2003), and others. However, the upregulation of H-RAS, C-MYC, and other oncogenes have been associated with transformation, or have a role in cancer initiation progress (Kelekar and Cole,

1987; Jiang et al., 2009). Conversely, TERT is not associated with cell cycle regulator proteins, thus TERT does not cause genetic instability, and its reactivation is necessary to escape from M2 (Bond et al., 1999; Rosler et al., 2004).

1.5. Additional strategies to cope the limited life-span of primary cells

The life-span of primary cultures seriously limits their use, several techniques have attempted to increase their proliferating capacity, and as immortalization of cells may cause insertional mutagenesis, cellular transformation or aneuploidy (Takeuchi et al., 2007; Balducci et al., 2014; Drayman et al., 2016). The cell reprogramming in an alternative, which attributes unlimited proliferative capacity and pluripotency to stem or somatic cells. For this purpose, the expression of pluripotency factors such as *Oct3/4*, *Sox2*, *c-Myc*, *Klf4*, and other transcription factors, has been utilized (Mathew et al., 2010; Takahashi et al., 2006). There are a lot of methods for reprogramming adult cells including retroviral, lentiviral, adenoviral, minicircle vectors, the novel technique CRISPR-associated protein (Cas) 9 system, and others have been used (Csobonyeiova et al., 2015; Liu et al., 2018). However, the use of some viral vectors is a long process that can include insertional mutagenesis and some factors that can affect the efficiency and specificity (Diecke et al., 2015; Peng et al., 2016).

Alternative methods have been used to expand the proliferative capacity of primary cultures. For example, the use of antioxidants as N-acetylcysteine, statin or atorvastatin can reduce the intracellular reactive oxygen species, and delay the

senescence of human endothelial cells *in vitro* (Haendeler et al., 2004). Furthermore, the use of conditioned extracellular matrix by young cells may enhance the proliferation of diploid human fibroblasts in culture and is sufficient for reverting of the senescence of these cells (Choi et al., 2011). Moreover, the use of medium conditioned by human embryonic stem cells, enhances the expansion of mesenchymal stromal cells in culture when they are cultivated under hypoxic conditions (Prasajak et al., 2015). Also, the xeno-free culture conditions, as the use of pooled allogeneic human serum can increase the proliferation of human adipose tissue-derived stem cells cultured (Paula et al., 2015), as well as other alternative methods have been developed (Conboy et al., 2005; Vatolin et al., 2019).

1.6. Strains, and cell lines used to study the human adipose tissue

Among the cellular models widely used to study the white human adipose tissue *in vitro,* we found the murine cell lines 3T3-L1 (Green and Kehinde, 1975), 3T3-F442A (Green and Kehinde, 1976), and the human SGBS strain (Wabitsch et al., 2001). The first two cell lines were derived from cloning of the mouse Swiss embryonic fibroblast 3T3 cell line, immortalized by routinely serial subculture (Todaro and Green, 1963). The 3T3-L1 cell line was the first preadipocyte cell line reported, and until now is the generally used model to study the adipogenesis *in vitro* by its easy handling in culture, its adipogenic potential and its availability to research community (Green and Kehinde, 1975; Lane et al., 1999). While the 3T3-F442A cell line was isolated also from 3T3 cells, but these cells display a more advanced commitment into the adipocyte lineage, and are capable of accumulating more fat than 3T3-L1, and can be differentiated in adipocytes *in vivo* (Ruiz-Ojeda

et al 2016; Armani et al., 2010). However, the molecular and metabolic differences with human adipose tissue of the first and second (Mikkelsen et al., 2010), and the abnormal tissue origin of the third (Wabitsch et al., 2001), disqualify these cells as optimal models. Furthermore, the anatomical origin of 3T3 cells is unknown, because they were derived from complete embryos non-discriminating between cells that could give origin to diverse organs (Jozefczuk et al., 2012). For that, all the cell lines derived from 3T3 cells display characteristics of brown and white adipocytes (Morrison and McGee, 2015).

The SGBS strain was derived from the stromal-vascular fraction of the subcutaneous adipose tissue of a cadaver of an infant with Simpson-Golabi-Behemil syndrome. SGBS is an X-linked congenital overgrowth disease; characterized by macrosomia, increase risk of embryonal cancer (Yeo et al., 2017). This syndrome may be originated by deletions or point mutations within the glypican 3 genes or by mutations in another currently unknown genes (Ruiz-Ojeda et al., 2016). SGBS strain is the only fully described preadipocyte cell line derived from humans, however, they do not show clear white or brown adipose tissue differentiation and therefore their cellular and identity remain uncertain (Yeo et al., 2017; Montanari and Colitti, 2018).

There are few human adipogenic cell lines that have been established. For example, Chub-S7 (Darimont et al., 2003), hASC-TE (Balducci et al., 2014), hMSC-hTERT-E6/E7 (Okamoto et al., 2002), others (Wolbank et al., 2009), which were derived from normal tissue, and had been immortalized by overexpression of SV40gp6, E7 or/and E6, in the different combinations using transduction method. Nevertheless, although these cell lines are from human origin, they are scarcely

used and non-used anymore, probably because they show low adipogenic potential, or have not been completely characterized. Furthermore, none of the human cell lines previously cited is easily available to the scientific community. The representative Tables 1, and 2 show the most frequently used cell lines in the study of adipose tissue *in vitro*, either derived from mice or human, respectively.

Table1. Murine cell lines widely used to study adipogenesis *in vitro*

Cell line	Soruce	Characteristics	Ploidy	Reference	Cites to date
3T3-L1	Murine Swiss 3T3 cells from embryos of 17 to 19 days	Can differentiate in mature adipocytes in culture medium with fetal bovine serum at 10%, dexamethazone, methylisobuthylxantine, and insulin	Aneuploid	Green H and Kehinde O, 1974	10028
3T3-F442A	Murine Swiss 3T3 cells from embryos of 17 to 19 days	Can differentiate in mature adipocytes in culture medium with fetal bovine serum at 10%, and insulin, has adipose commintent by growth arrest	Aneuploid	Spiegelman BM, et al, 1983	527
OP9	Mouse bone marrow derived stromal cells	Can be differentiated in 72 h with insulin oleate media	Unknown	Wolins, et al, 2005	183
3T3-A31	Murine BALB/c	Can be transformed easily	Aneuploid	Aaronson SA, and Todaro GJ, 1968	102
Ob17	Murine epididymal fat pads	Derived from genetically obese murine adults (ob/ob)	Unknown	Gharbi-Chichi J, 1981	41

Table2. Human cell lines to study adipogenesis *in vitro*

Cell line	Source	Characteristics	Ploidy	Reference	Cites to date
PAZ6	Stromal vascular fraction of brown adipose tissue	Immortalized by overexpression of SV40gp6. Can differentiate in mature adipocytes in ITT medium by addition of biotin, phatothenate acid, dexamethasone, insulin, methylisobuthylxantine, pioglitazone, and triiodothironine.	Unknown	Zilberfarb, et al, 1997	13
Chub-S7	Subcutaneus cells from abdomen	Immortalized by overexpression of *hTERT y* E7, has achieve 176 PDLs, has a doubling time of 45.6 ± 0.8 h. Can differentiate in mature adipocytes by addition of biotin, phatothenate acid, dexamethasone, insulin, transferrine, methylisobuthylxantine, rosiglithazone, fetuin, and triiodothironine.	Diploid	Darimont, et al, 2003	13
ASC52telo	Subcutaneous adipose tissue	Immortalized by overexpression of TERT, has achieved 65 PDLs, has a doubling time of ~45 h, and is multipotent. Can differentiate in mature adipocytes by addition of fetal calf serum at 10% L-glutamine, dexamethasone, insulin, indomethacin, and methylisobuthylxantine.	Diploid	Wolbank, et al, 2007	2
hMSC-hTERT-E6/E7	Mesenchymal stromal cells	Immortalized by overexpression of *hTERT y E6/E7, has achieved 80PDLs, and is multipotent.* Requires 3 cycles of induction-maintainment to differentiate in mature adipocytes by addition of fetal bovine serum at 10%, dexamethazone, methylisobuthylxantine, insulin, and indometacine.	Unknown	Okamoto, et al, 2002	0
hASC-TE	Subcutaneus cells from abdomen	Immortalized by overexpression of TERT, E6/E7, has a doubling time of 39.1 ± 4.2, and has not been completely characterized. Can differentiate in mature adipocytes by addition of NH AdipoDiff medium.	Aneuploid	Balducci, et al, 2014	0
hASC-TS	Subcutaneus cells from abdomen	Immortalized by overexpression of TERT, SV40gp6, has a doubling time of 32.1 ± 8.5 h, and has not been completely characterized. Can differentiate in mature adipocytes by addition of NH AdipoDiff medium.	Aneuploid	Balducci, et al, 2014	0

2. Justification

The lack of adequate *in vitro* models to study human adipogenesis has led to the necessity for development of permanent or high extensible models that efficiently permit the analysis of white human adipose tissue physiology and molecular biology. IPI-SA3-C4 population is a candidate model to study the human adipose tissue *in vitro*, however its limited lifespan is the main drawback. Therefore this work was carried out to characterize and establish the conditions for long-term culture of these cells.

3. Aims of the study

- To characterize the proliferative and differentiation capacities of the human subcutaneous preadipocyte cells designated as “IPI-SA3-C4”.
- To analyze the expression of stem cell markers in IPI-SA3-C4 cells and determine both karyotype and tumorigenic potential.
- To study the effects on cell proliferation and adipogenic potential when IPI-SA3-C4 cells are cultivated onto extracellular matrix substrata and/or supplemented with medium conditioned by human embryonic stem cells alone.

4. Materials and methods

4.1. Isolation of IPI-SA3-C4 cells

An inguinal subcutaneous adipose tissue sample was obtained from a male patient (20 months old) attended for corrective surgery of syndactyly in The Woman and Child Hospital (San Luis Potosí, México) with the Parent informed consent and the approval of the Hospital Ethics Committee. Primary cultures of adipose stromal-vascular cells were established and passaged as described (Herrera-Herrera et al. 2009). At the 10th passage, a clonal population, designated as IPI-SA3-C4 (Clone 4 obtained from the third human subcutaneous adipose tissue sample processed at IPICYT), was isolated from a low-density culture (one cell per well in 24-well plates).

4.2. Culture of IPI-SA3-C4 cells

IPI-SA3-C4 cells from 13th passage (~46 Population doubling number (PDLs)) were cultured on standard culture medium (basal medium; BM): L15-Leibovitz (Sigma) supplemented with 10% of fetal bovine serum, or 5% fetal bovine serum (FBS), 5% calf serum (both from HyClone), and penicillin 80 U/mL and streptomycin 80 µg/mL.

To evaluate the effects of growth IPI-SA3-C4 cells on uncoated or Matrigel®-coated cell culture dishes; or on extracellular matrix conditioned by hESC, the hESC line H9 was cultured for 4 days and cells were removed using 0.5M EDTA.

The hESC-conditioned medium was harvested the same day of the culture medium change and diluted in BM.

For short-term growth assays cells were seeded at 5.3 x10^3 cells/cm^2 and counted every 24 or 48 hours for 10 or 14 days. Doubling time T(d) = 48h/log2 (N_2/N_1), (N_1- initial cell count; N_2 - cell count after 48 hours) (Suga et al., 2007).

For long-term growth assay the cells were seeded at 3.4 x10^3 cells/cm^2. Every 3 or 4 days the cells were harvested, counted, and reseeded at initial cell density. PDL = log (Nn / Nn-1) / log2, (n – passage number; N - number of cells) (Böcker et al., 2008).

For colony-forming assay 100 IPI-SA3-C4 cells were seeded per 60 mm diameter culture vessel. After 15 days the vessels were fixed in 3.7% formaldehyde, stained with Harris hematoxylin (Jalmek) and counted. An independent cell group larger than 50 cells was considered a colony.

For hTERT inhibition assay the IPI-SA3-C4 cells were seeded at 2.6 x10^3 cells/cm^2 and 60 µM Telomerase Inhibitor BIBR1532 (BIBR; Sigma) was added to the growth medium. Equal volume of dimethyl sulfoxide (DMSO; Sigma) was used as a control. Cells were stained with trypan blue and live cells were counted on days 1, 3, 5, 7 and 9 using a hemocytometer.

4.3. Adipogenic differentiation

To evaluated the adipogenic capacity of IPI-SA3-C4 cells, confluent cultures were induced to adipose differentiation with adipogenic medium (AM; L15 medium

(Sigma) containing 10% FBS, 100 nM insulin, 33 µM biotin, 17 µM calcium pantothenate, 100 nM cortisol, transferrin 5 µg/mL, 2 nM triiodothyronine, 100 nM dexamethasone, 500 µM isobutyl-methyl-xanthine (all from Sigma) and 1 µM Rosiglitazone (Cayman Chemical) for six days. Cultures were maintained for 15 additional days in maintenance medium (MM; AM lacking dexamethasone, isobutyl-methyl-xanthine and Rosiglitazone).

The Glyceraldehyde 3-phosphate dehydrogenase (GPDH) activity was determined by mixing 10 µg total cellular protein obtained from non-differentiated or adipose-induced IPI-SA3-C4 cells with 2 mM phosphate dihydroxyacetone phosphate (Sigma). The mix was incubated for 2 minutes at room temperature and transmitting light absorbance at 340 nm was measured using a plate reader Epoch (Biotek) (Herrera-Herrera et al. 2009). The glucose uptake was determined by incubating terminally differentiated IPI-SA3-C4 adipocytes with the fluorescent glucose analog 2-[N-(7-nitrobenz-2-oxa-1,3-diazol-4-yl)amino]-2-deoxy-D-glucose (2-NBDG; Invitrogen) as previously described (Alonso-Castro et al. 2011). For Oil Red O and Nile Red/DAPI staining, the cell monolayers were fixed with 3.7% formaldehyde for 20 min at 4°C. Cultures were then incubated with either a saturated 2-propanol solution of Oil Red O overnight or with Nile Red 1 µg/mL and 4',6-diamidino-2-phenylindole (DAPI) 1 µg/mL (all reagents from Sigma) for 15 min (Aldridge et al. 2013). Oil Red O-stained adipocyte clusters per dish were quantified manually under microscopy. Nile Red and DAPI were measured with a multimodal detector (Beckman Coulter), or multimode microplate reader Infinite M200 PRO (TECAN) at λ_{ex} = 485 nm and λ_{em} = 535 nm for Nile Red and λ_{ex} = 360 nm and λ_{em} = 430 nm for DAPI (Aldridge et al. 2013). Readings were obtained

before and after the staining procedure and non-stained wells were used to measure background fluorescence. In parallel, representative micrographs of dyed cells were taken using fluorescence microscopes, Axio imager M2 Carl-Zeiss, or Olympus BX71 and processed with Hokawo v2.1 (Hamamatsu Photonics) software. Quiescent IPI-SA3-C4 cells maintained in BM were used as negative controls for the listed experiments.

4.4. Osteogenic differentiation

To evaluated the osteogenic capacity of IPI-SA3-C4 cells, confluent cultures were incubated in osteogenic induction medium (OM; L15 medium supplemented with 10% FBS, 10 nM dexamethasone, ascorbic acid 50 µg/mL, 10 mM β-glycerophosphate and antibiotics) for three weeks. The cells were subsequently stained with leukocyte alkaline phosphatase kit (Sigma) according to manufacturer's instructions. Parallel cultures were fixed with 3.7% formaldehyde for 20 min at 4°C and incubated in 10% Alizarin Red (Sigma) solution for 20 min with slow agitation (Birmingham et al. 2012). Then cells were incubated in 800 µL of 10% acetic acid for 30 min at room temperature, the cell monolayers were transferred to Eppendorf tubes, mixed vigorously, heated at 85°C for 10 min and centrifuged at 13,000 rpm for 15 min. Five hundred microliters of the supernatant was passed to a new tube and 200 µL of 10% ammonium hydroxide was added. The absorbance was measured in a plate reader Epoch (Biotek) at 405 nm (Gregory et al. 2004). To measure the alkaline phosphatase activity total protein was extracted from cells using 1% Triton X-100 (Sigma) in cold PBS. The total protein concentration was measured using standard Bradford method. Next, 10 µg

of total protein was mixed with 50 µL of 0.5 M 2-amino-2methyl propanol (Sigma), 2 mM $MgCl_2$ (Promega) at pH 10 and 10 mM p-nitrophenyl phosphate (Chemicon) and incubated during 40 min at 37°C. The absorbance was measured in a plate reader Epoch (Biotek) at 405 nm and the alkaline phosphatase activity was calculated as follows:

Activity = volume (µl) * ($AbsT_o$ – $AbsT_n$) cm^{-1} / αM 405nm p – nitrophenol * time * µg protein; where $1.78x10^4$ M^{-1} cm^{-1} is the molar extinction coefficient for p-nitrophenol at 405 nm (αM405nm) (Sabokbar et al. 1994).

4.5. Chondrogenic differentiation

To evaluate the chondrogenic capacity of IPI-SA3-C4 cells, micromass cultures of IPI-SA3-C4 cells were established by seeding 4 $x10^5$ cells/µL in 35 mm dishes (four micromasses per dish) with BM and incubating overnight. Next, cultures were incubated in either 2 mL of chondrogenic medium (CM; L15 medium, 1% FBS, 50 nM ascorbic acid, TGF-β1 10 ng/mL (PeproTech), insulin 6.25 µg/mL (Sigma) and antibiotics) or BM (controls) for three weeks (Ahrens et al. 1977; Denker et al. 1995). Micrographs of micromass cultures were taken at 24 h and 21 days after plating and the diameters of cultures were measured using ImageJ software. The chondrogenesis efficiency was quantified by subtracting the diameter of the micromass the first day from that measured at 21st day. To detect glycosaminoglycans, the cultures were dyed with 1% Alcian Blue solution (Sigma) in concentrated HCl on day 21 (Denker et al. 1995).

4.6. Karyotyping

To determinate in first instance if IPI-SA3-C4 cells are normal or not, we exponentially growing IPI-SA3-C4 cells at the 20th, or 10th passage were treated with colchicine 0.1 µg/mL (Sigma) for 1 h at 37°C. Subsequently, the cells were harvested and treated with 0.075 M KCl and a 3:1 methanol-glacial acetic acid for 20min. Chromosome preparations were obtained by dropping cell suspensions on cold wet coverslips and subsequent staining with 1:20 Giemsa solution (Sigma) for 5 min (Stultz et al. 2016). Alternatively, chromosomes preparations were used for G banding, to immerse the slides in trypsin for 10 seconds, washing three times in alcohol and staining with Giemsa solution for 10min. The chromosome preparations were analyzed visually using a bright-field microscope, or using the IKAROS program.

4.7. Soft agar colony formation assay

The soft agar colony formation assay is a well-established method for evaluating transformation *in vitro*. For that, 6 wells-plates were used to plate the bottom and top layers of noble agar (final concentration 0.5%, and 0.3%, respectively), where 2x L15 medium supplemented with FBS at 20% was utilized as diluent. Before to diluted the noble agar all the reagents were maintained at 42 °C to avoid premature hardening, and after to plate 1.5 ml noble agar solution for the bottom layer, the plates were maintained by 30 min at room temperature, same event was developed for plate the top layer which contains the cells to use (Borowicz, 2014). Where, IPI-SA3-C4 cells from passage 19, and positive control HeLa cells were

seeded at 5000 cells/well. Additional 100 µl of L15 medium was added over the top layer twice weekly to prevent desiccation. All the cultures were incubated at 37°C in a humidified atmosphere, in a camera with free gas exchange by 21 days. At the end of the experiment, manual counts were develop, and micrographs were taken.

4.8. Xenograft assay

Proliferating IPI-SA3-C4 cells (2×10^6, passage 19) or HeLa cells (2×10^6) were injected subcutaneously to the right flank of female athymic nude (Foxn1nu/nu) mice, three mice in each group. Fourteen days post implantation, the mice were sacrificed by cervical dislocation and injection sites were evaluated for tumor formation.

4.9. β-Galactosidase staining

To evaluate if IPI-SA3-C4 cells were senescent, the senescence-associated β-galactosidase activity was measured by staining the cells with Senescence Cells Histochemical Staining Kit (Sigma) in accordance with manufacturer instructions, and the percentage of labeled cells was evaluated under a bright-field microscope. Alternatively, other method was used, where cultures of IPI-SA3-C4 were fixed in 2% paraformaldehyde at room temperature for 10 min, rinsed 2x15 min in rinse buffer (2 mM $MgCl_2$, 0.02% NP40 in PBS) and incubated in staining solution (5mM $K_3Fe(CN)_6$, 5mM $K_4Fe(CN)_6$, 1mg/mL Xgal in rinse buffer) overnight (Klaas et al., 2019).

4.10. Reverse transcription-polymerase chain reaction

To evaluate the genic expression of IPI-SA3-C4 cells, end-point RT-PCR was developed, where RNA of IPI-SA3-C4 cells was isolated using TRIzol® (Invitrogen) according to manufacturer's instructions. The RNA was quantified in a spectrometer Epoch (BioTek) and its integrity was evaluated by electrophoresis. Total RNA (1 µg) was reverse-transcribed in a 25 µL volume reaction containing 4 µL reverse transcriptase (RT) buffer (50 mM Tris-HCl, 75 mM KCl, 3 mM $MgCl_2$ and 10 mM DTT), 0.5 mM dNTPs, 25 U RNasin and 10 U of Moloney murine leukemia virus RT for 90 min at 42°C. The RT was omitted in negative control reactions. cDNA was amplified by PCR in a reaction volume of 15 µL, containing 300 ng cDNA, 200 µM dNTPs, 1.5 mM $MgCl_2$, 1.25 U Taq DNA polymerase and 0.2 µM of specific oligonucleotides. All reagents were from Promega.

Alternatively, real-time RT-PCR was developed, where RNA was isolated using TRIzol® (Invitrogen), and subsequently purified with Nucleospin RNA Kit (Macherey-Nagel) according to the manufacturer's instructions. Total RNA was reverse transcribed with a RevertAid First Strand cDNA Synthesis Kit (Thermo Scientific) according to the manufacturer's instructions. qPCR was performed using Lightcycler 480 II (Roche). The primer sequences used are listed in Table S1. *GAPDH* expression level was used for normalization.

Table S1. Primers used for RT-PCR

Gene	Sequence	Amplic(pb)
ACAN	fw AGCAGTCACACCTGAGCAGCA rv CCGATCCACTGGTAGTCTTGGGCA	82
ATF4	fw GAGGATGCCTTTTCCGGGACAG rv GAGATGGCCAATTGGGTTCACTG	207
ALPL	fw. ACCAATGCCCAGGTCCCTGACA rv. GTGGCATGGTTCACTCTCGTGG	212
BMP7	fw. CTCAATGCCATCTCCGTCCTC rv. GGATCTTGTTCATTGGATGCTGCC	300
CEBPA	fw. ACTGAGTAGGGGGAGCAAATCGTG rv. GTTCCAAGCCCCAAGTCCCTATG	220
CEBPB	fW. CCGTGGACAAGCACAGCGACGAGTA rv. CAGCTGCTTGAACAAGTTCCGCAG	206
CEBPD	fw. CGAGCGCAACAACATCGCCGTG rv. GTTACCGGCAGTCTGCTGTCC	218
COL1A1	fw. CCCCTGGAAAGAATGGAGATG rv. TCCAAACCACTGAAACCTCTG	148
COL2A1	fw. GTCTTGGTGGAAACTTTGCTGCC rv. ACACCAGGTTCACCAGGTTCA	184
FABP4	fw. CAGTGTGAATGGGGATGTGA rv. GTGGAAGTGACGCCTTTC	249
GAPDH	fw. GAAGGTGGTGAAGCAGGCGT rv. ATGTGGGCCATGAGGTCCACCA	216
KLF4	fw. CTGCTCCCATCTTTCTCCAC rv. GTTGAACTCCTCGGTCTCTC	234
LEP	fw. ACACGCAGTCAGTCTCCT rv. AGGTTCTCCAGGTCGTTG	172
LIN28A	fw. CGTGTCCAACCAGCAGTT rv. TTGAACCACTTACAGATGCCC	100
MYC	fw. TCGGATTCTCTGCTCTCCTC rv. CGCCTCTTGACATTCTCCTC	413
NANOG	fw. GCCTCAGCACCTACCTAC rv. GCAGCCTCCAAGTCACT	270
POU5F1	fw. GAGAACCGAGTGAGAGGCAA rv. CAGAGTGGTGACGGAGACAG	320
PPARG	fw. ATGGGTGAAACTCTGGGAGA rv. TGGAATGTCTTCGTAATGTGGA	246
RUNX2	fw. GATCTGAGATTTGTGGGCCGGA rv. TGGGATGAGGAATGCGCCCTAA	217

SOX2	fw. ATGTCCTACTCGCAGCAG rv. CTCTGGTAGTGCTGGGA	200
SOX9	fw. CCTCAAAGGGTATGGTCATCTGTT rv. TAGCCTCCCTCACTCCAAGA	386
TERT	fw. TGTCCCTGAGTATGGCTGCGT rv. TGAGACTGGCTCTGATGGAGGTCC	206

4.11. Immunofluorescence analysis

To visualize the expression of specific proteins by immunofluorescence, IPI-SA3-C4 cells were seeded on coverslips with BM, or were seeded on uncoated or Matrigel®-coated coverslips, and maintained for 72 h at 37°C in a humidified atmosphere of free-gas exchange. Then, cells were fixed with 4% paraformaldehyde and 0.1% Triton-X-100 for 10-15 min at room temperature, blocked with 4% normal goat serum and incubated with primary antibodies Alexa Fluor® 647 Mouse anti-Oct3/4 or PerCP-Cy™5.5 Mouse anti-Sox2 (BD Biosciences), or with hTERT antibody (1:100 LS-B11086, LSBio) overnight at 4°C, followed by incubation with Alexa-488 conjugated goat anti-rabbit secondary antibody (1:100 Life Technologies) for 1h at room temperature. Cell nuclei were stained with DAPI (Sigma; 1 µg/mL). Positive cells were quantified by manual counts of >300 cells per preparation. Images were acquired with an Olympus BX-71 fluorescence microscope and processed with Hokawo v2.1 (Hamamatsu Photonics) software.

4.12. Telomere length quantification

To determinate if hTERT was or not active in IPI-SA3-C4 cells, cultures from the passage 1 and 20 were seeded at 2.32 $x10^3$ cells/cm^2, and genomic DNA was

extracted 72 h later. The cells were lysed in 100 mM NaCl, 10mM Tris pH8, 25mM EDTA pH8, 0.5% SDS and 400 µg/mL. Next, the lysates were incubated at 56°C for 1 h, and genomic DNA extraction was accomplished by Trizol-chloroform treatment according to the manufacturer's instructions. Subsequently human telomere length quantification qPCR assay kit (Sciencell) was used according to the manufacturer's instructions.

4.13. Statistical analysis

All experiments were performed at least in triplicate. The results are presented as the mean ± standard deviation. GraphPad Prism 6 program was used to analyze the data by Student’s t-test and the differences were considered statistically significant when $P < 0.05$ or $P < 0.01$.

5. Results

5.1. Characterization of IPI-SA3-C4 cells as a suitable model for adipogenesis *in vitro*

Currently, there is not a generally accepted *in vitro* model to study human adipose tissue, because the *in vitro* models more used to analyze adipose tissue consist in cell lines with a murine origin, and hence, with genetic and metabolic differences with human adipocytes. Here, we characterized human preadipocyte cells, which were derived from primary cultures of adipose stromal-vascular cells. These primary cultures were obtained from an inguinal subcutaneous adipose tissue sample from a male patient (20 months old) after a corrective surgery of syndactyly. At the 10th passage, a clonal population, designated IPI-SA3-C4 (Clone 4 obtained from the third human subcutaneous adipose tissue sample processed at IPICYT), was isolated from a low-density culture (one cell per well in 24-well plates), in conjunction with other clones. The preliminary assays to evaluate IPI-SA3-C4 cells potential to proliferate and differentiate in adipocytes, revealed that these cells fulfil the characteristics necessary for being characterized and convert them in a useful model of human adipose tissue. Our results showed that IPI-SA3-C4 cells retained the proliferation capacity *in vitro* for up to 36 serial passages and 70 PDLs clearly exceeding the Hayflick limit showing more or similar proliferative potential to other systems (Fig. 1A) (Böcker et al., 2008; Balducci et al., 2014; Trivanović et al., 2015; Herrera-Herrera et al., 2009). Their duplication time at the 17th passage was 50 ± 4 h, which is shorter than the reported for similar cell populations (Fig. 1B) (Herrera-Herrera et al., 2009; Balducci et al.,

Figure 1. Cell growth properties of IPI-SA3-C4 cells.

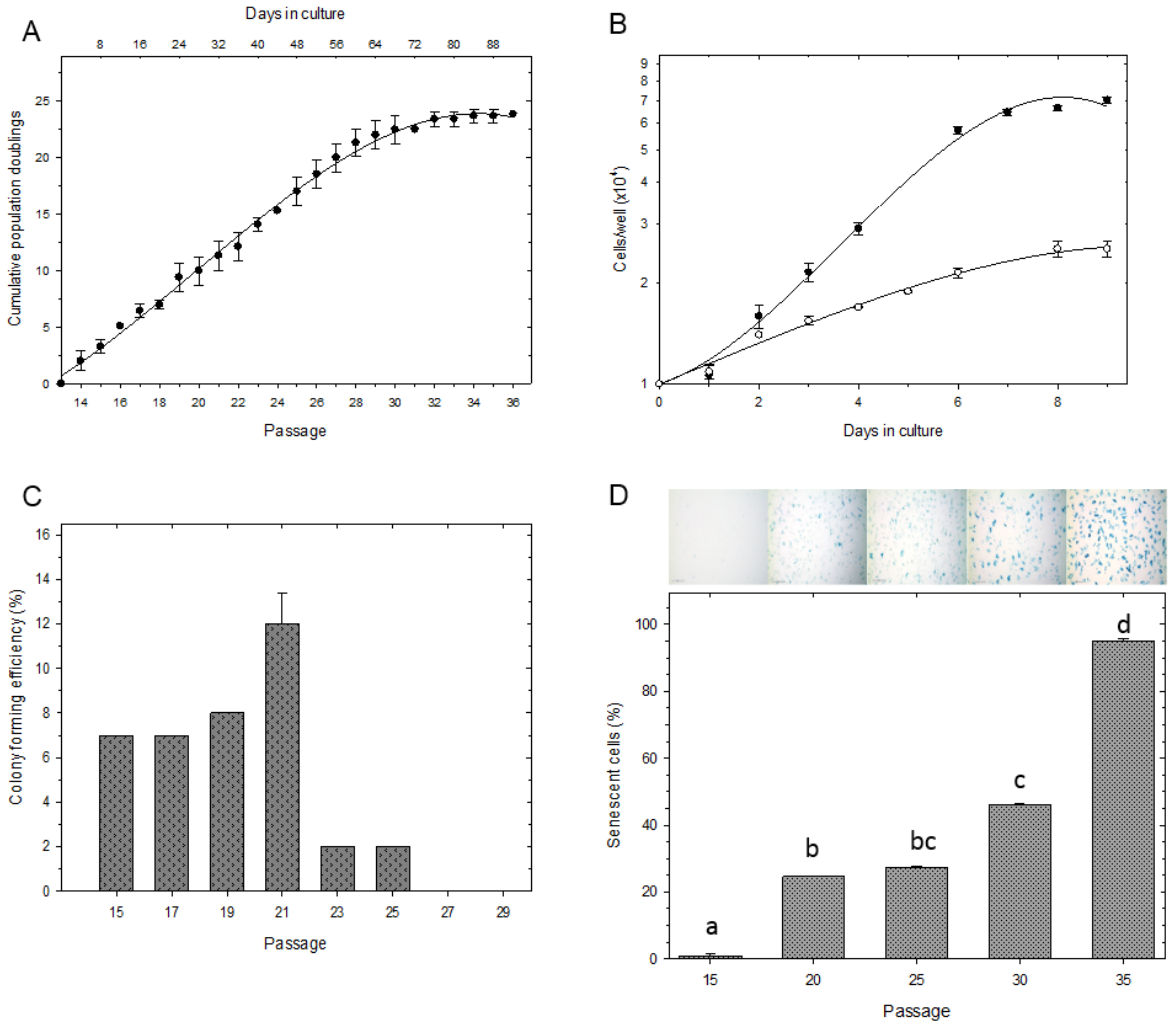

2014; Trivanović et al., 2015) or longer than others (Wabitsch et al., 2001; Darimont et al., 2003). Moreover, the colony forming efficiency of IPI-SA3-C4 cells isolated at passages 15, 17, 19, 21, 23, and 25 was 7%, 7%, 8%, 12%, 2%, and 2%, respectively (Fig. 1C). However, IPI-SA3-C4 cells entered at growth arrest after 70 PDLs, and the percentage of senescent cells was gradually elevated as the cells were subcultured, suggesting the induction of senescence during their *in vitro* cultivation, as usually happens in normal human cells (Fig. 1D). On the other hand, IPI-SA3-C4 cells expressed pluripotency markers such as KLF4, OCT4, NANOG, and MYC at early subcultures (Fig. 2A); also the presence of the OCT4 protein was revealed by fluorescence analysis at passage 19 (Fig. 2B), but not at passage 24 (Fig. 2C). The fractions of POU5F1 and SOX2 expressing IPI-SA3-C4 cells were 16.16% ± 4.24 and 8.69% ± 3.53, respectively, at the 19th passage, and 0.33% ± 0.5 and 0.29% ± 0.44, respectively, at the 24th passage (Fig. 2D). Furthermore, IPI-SA3-C4 cells retained a normal chromosomal complement as diploid population (Fig. 3A). Also, we evaluated the ability of IPI-SA3-C4 cells to growth on soft agar and to develop tumors as xenografting. After 15 d in culture, IPI-SA3-C4 cells plated on polystyrene showed a strong increase in cell density whereas IPI-SA3-C4 cells grown on soft agar showed no proliferation (Fig. 3B). In contrast, the transformed HeLa cell line showed a clear clonal growth under both culture conditions (Fig. 3B). In the same manner, IPI-SA3-C4 cells grafted in nude mice did not form solid tumors (Fig. 3C-II) while HeLa cells formed tumors of ~7 mm diameter in nude mice (Fig. 3-I). Moreover, IPI-SA3-C4 cells possess also a high potential for differentiation into adipocytes; surprisingly IPI-SA3-C4 cells expressed the early adipogenic markers KLF4, CEBPB and CEBPD in stages

Figure 2. Expression of stemness markers by IPI-SA3-C4 cells.

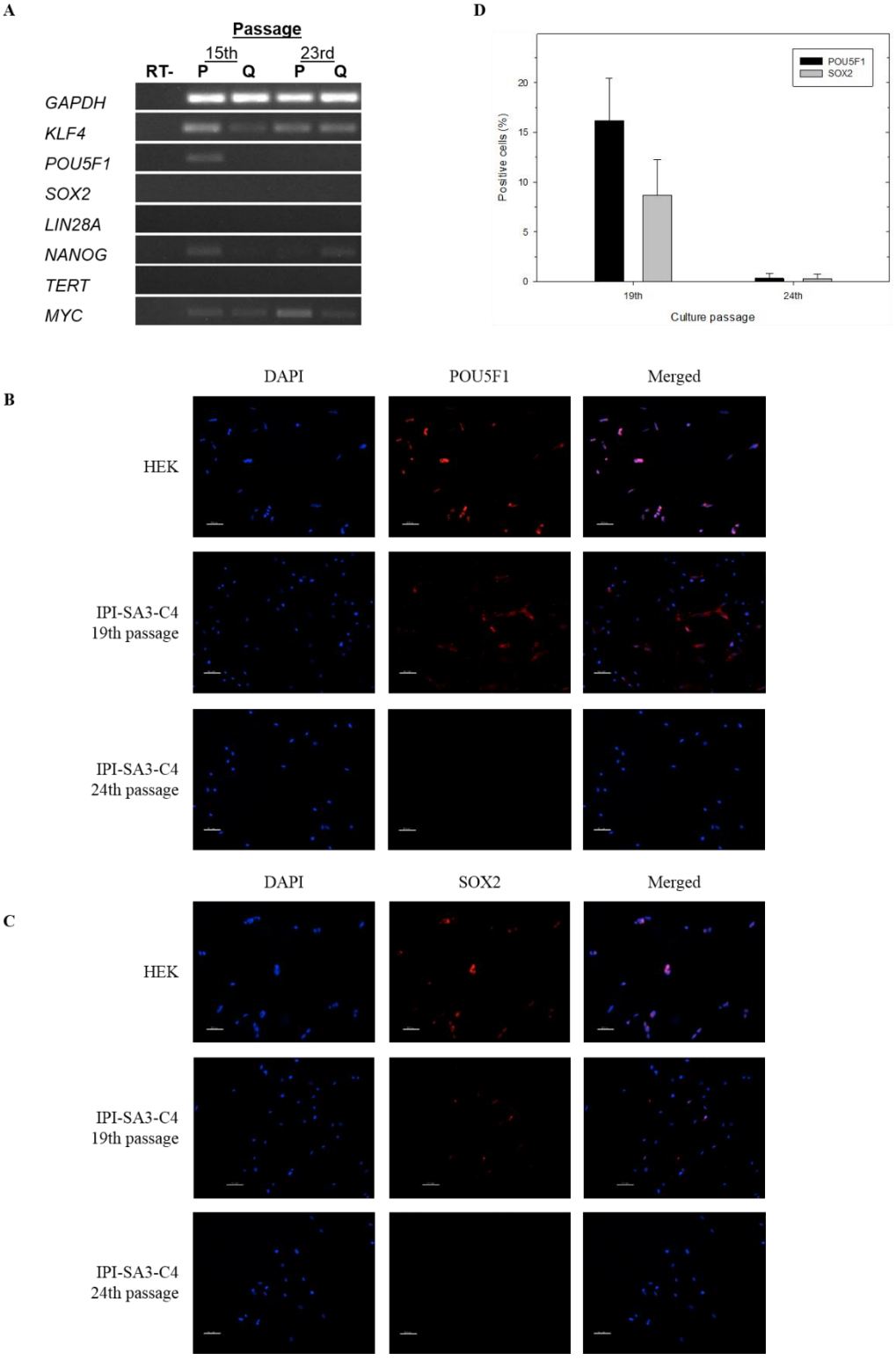

Figure 3. Karyotype and tumorigenesis analysis of IPI-SA3-C4 cells.

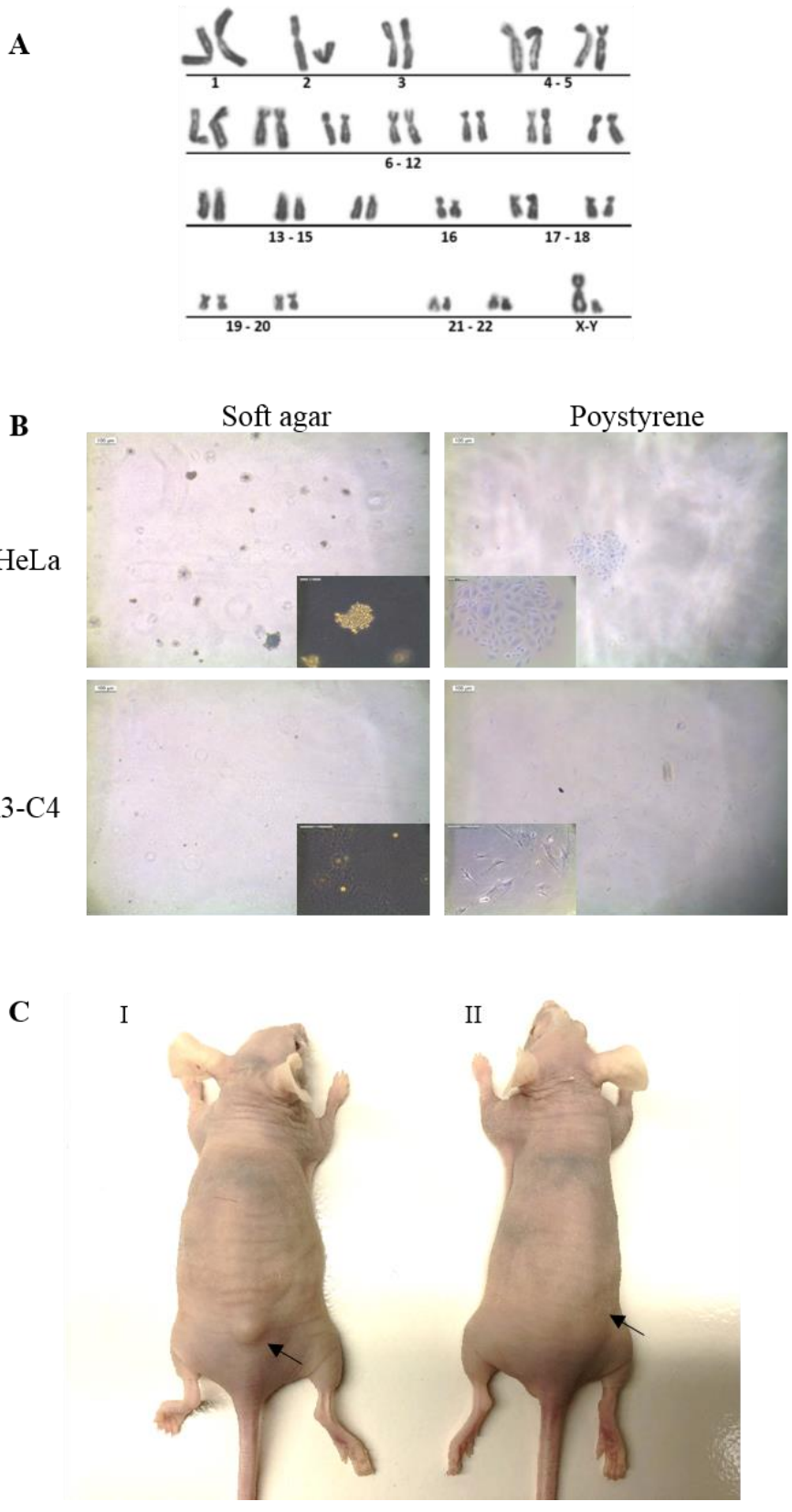

previous to induction (Fig. 4A), similar to 3T3-F442A cell line, pointing to its inherent preadipocyte nature. Intracytoplasmic triglyceride accumulation is the most conspicuous cellular feature in terminal adipogenesis. Figure 4B shows that quiescent non-induced IPI-SA3-C4 cells (Fig. 4Ba, Bb) did not accumulate triglycerides while adipose-induced cells did (Fig. 3c), as evidenced by the specific staining with Nile Red (Fig. 4Bd). Cells in Fig. 4Bb and Bd were also stained with DAPI to evidence cell nuclei.

Labeling of intracellular lipids with Nile Red and Oil Red O was used to characterize the maturity of adipocyte differentiation. The Nile Red staining of IPI-SA3-C4 cells of 15th and 23rd passages induced to differentiate into adipocytes was increased 29.56 ± 0.01 and 9.50 ± 0.06 times, respectively, when compared to non-treated cells. The number of Oil Red O positive differentiation clusters derived from IPI-SA3-C4 cells of 15th and 23rd passages induced to differentiate into adipocytes was 103 ± 2 and 33 ± 1 per plate, respectively (Fig. 4C). Further, we measured the activity of GPDH enzyme, which is essential for triglyceride and is present in differentiated adipocytes. The GPDH enzyme activity in IPI-SA3-C4 cells of 15th and 23rd passages induced to differentiate into adipocytes was 0.0268 ± 0.0043 and 0.0107 ± 0.0026 U per milligram of total protein, respectively (Fig. 4D), demonstrating the presence of active GPDH. Finally, the activity of the insulin-responsive glucose transport system that is instrumental for adipocyte functioning was determined by the 2-NBDG uptake assay in IPISA3-C4 cells of 15th and 23rd

Figure 4. Adipogenic capacity of IPI-SA3-C4 cells at early and late passages.

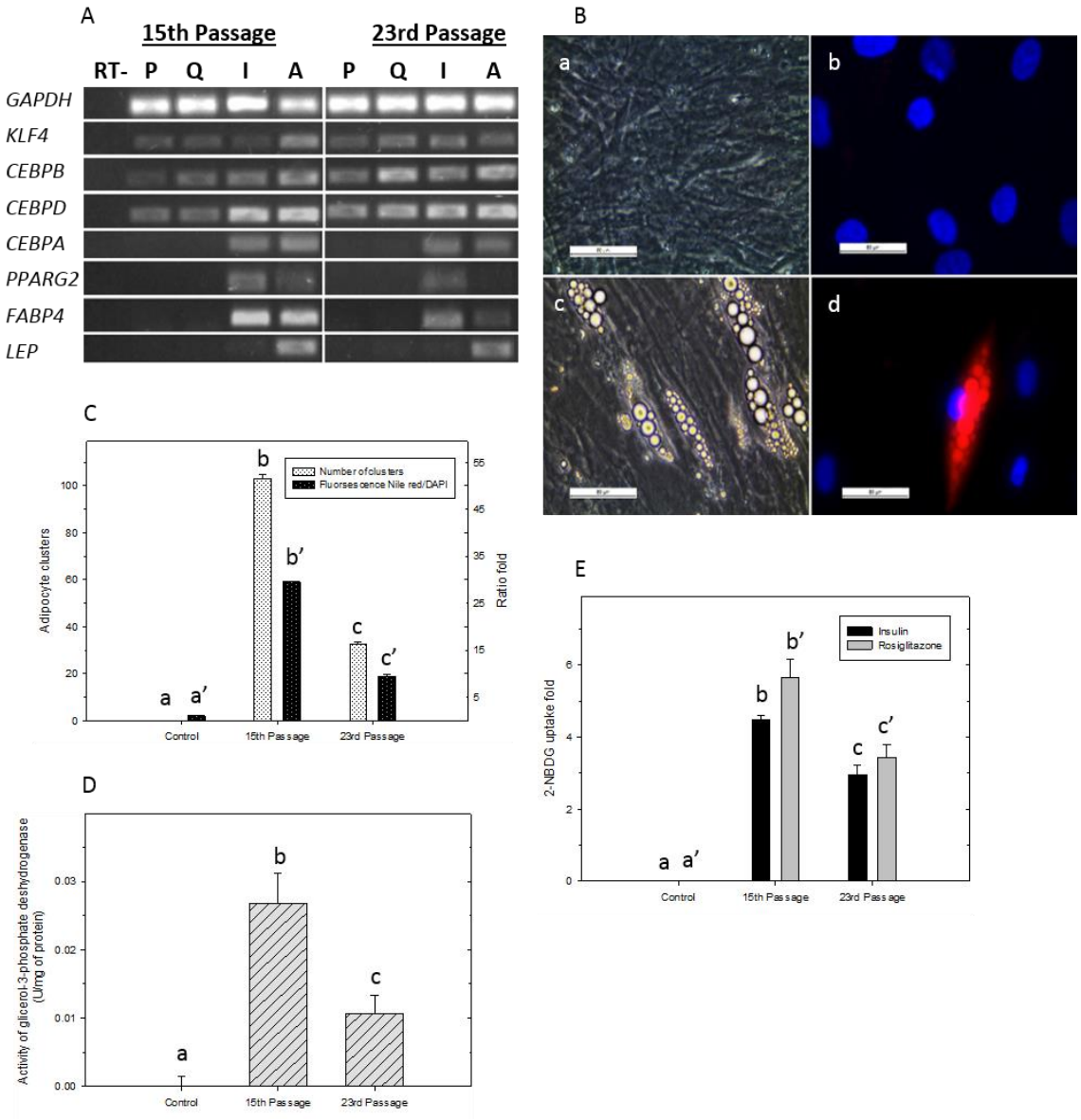

passages induced to differentiate into adipocytes. The 2-NBDG uptake was increased in these cells by 4.49 ± 0.11 and 2.95 ± 0.26 times when insulin was added and 5.66 ± 0.48 and 3.43 ± 0.34 times when rosiglitazone was added, respectively (Fig. 4E).

Furthermore, IPI-SA3-C4 cells can differentiate into osteoblasts (Fig. 5), and chondrocytes (Fig. 6), we ignored whether these cells undergo differentiation into other cell lineages. Also, these cells maintained their adipogenic potential even at passage 66 CPD, possessing a substantial advantage over current *in vitro* models for human adipogenesis. IPI-SA3-C4 cells showed characteristics of mesenchymal stromal cells, as well as high proliferative and differentiation capacities, same that lead us to propose its use as an adequate and alternative model to study the adipogenesis *in vitro*, although it has a limited life-span.

Figure 5. Osteogenic capacity of IPI-SA3-C4 cells at early and late passages.

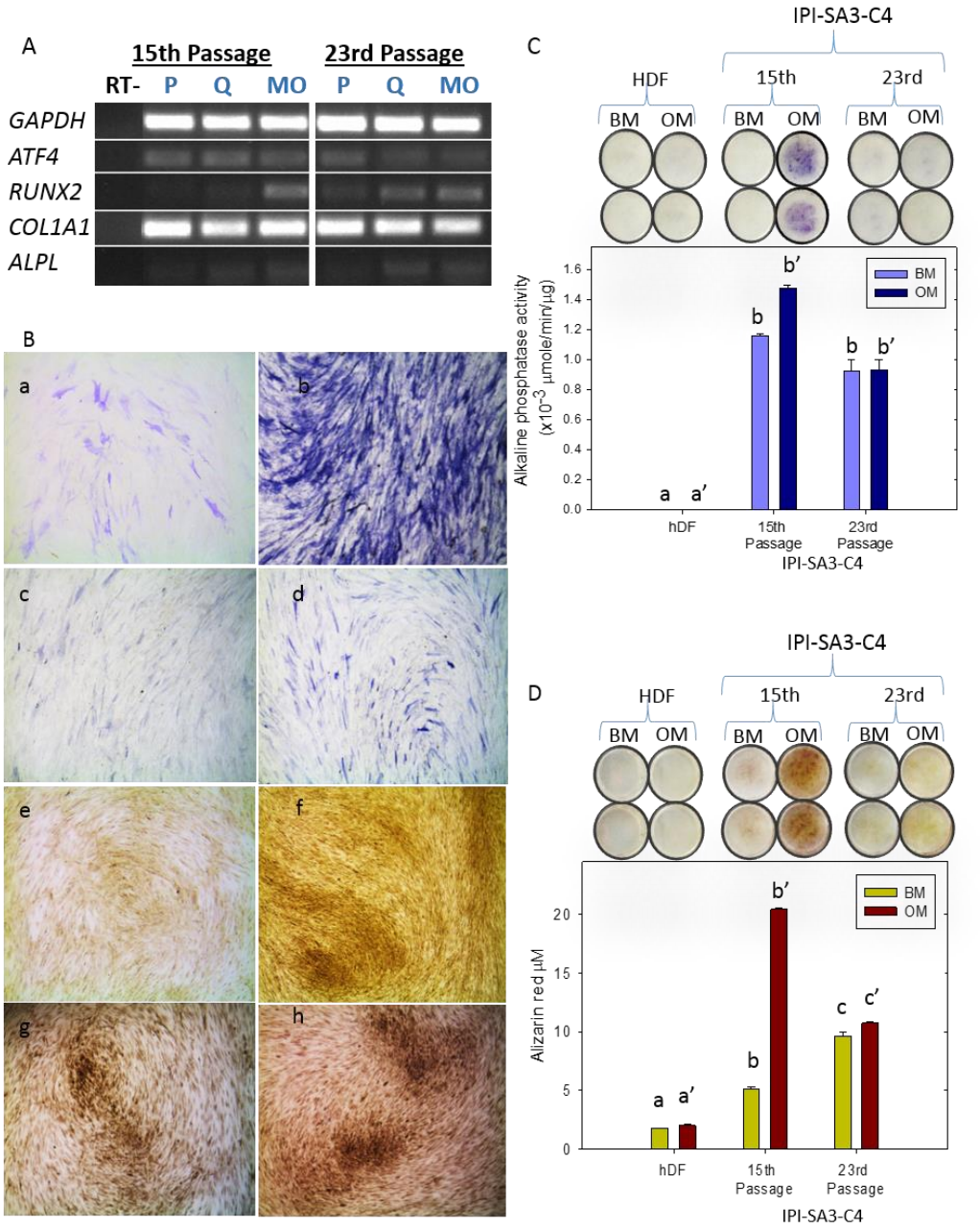

Figure 6. Chondrogenic capacity of IPI-SA3-C4 cells at early and late passages.

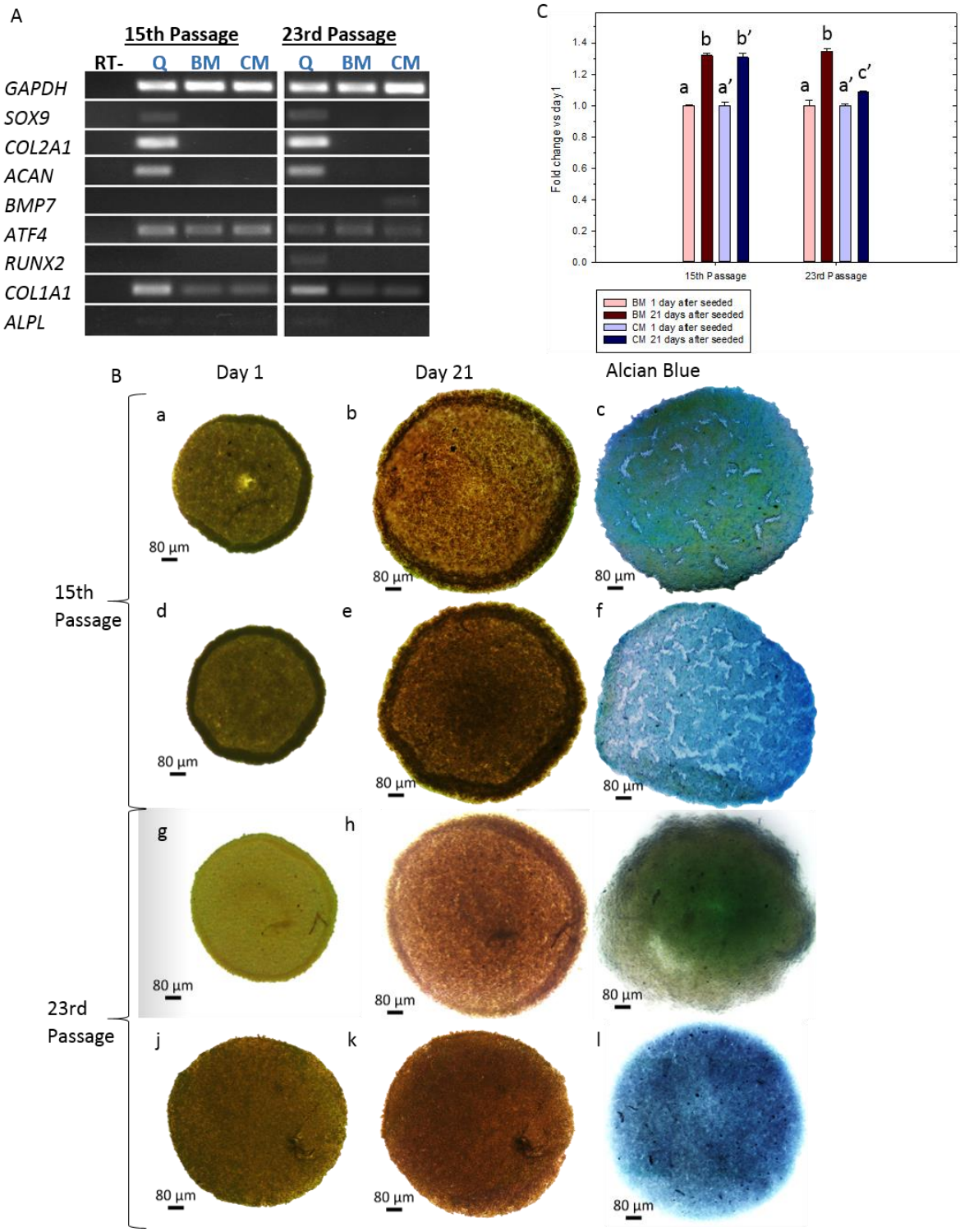

5.1.1 Figure legends

Figure 1. Cell growth properties of IPI-SA3-C4 cells. For long-term culture, IPI-SA3-C4 cells at the 13th passage were serially passaged by seeding 3.4 x10^3 cells/cm^2, harvesting them at the fourth day of culture, as they reached 80-90% of confluence, and then replating at the initial cell density (**1A**). The growth rate of IPI-SA3-C4 cells in 17th (●) and 26th (◌) serial passages was calculated by cell counting of cell suspensions in a hemocytometer (**1B**). The colony-forming efficiency of IPI-SA3-C4 was evaluated in low-cell density (100 cells/60 mm plate) considering a colony as any independent cell group larger than 50 cells (**1C**). Senescent IPI-SA3-C4 cells were quantified by assaying senescence-associated β-galactosidase activity at indicated passages. Micrographs upon the graph illustrate the senescent cells in each passage (**1D**). All the cultures were incubated at 37°C in a humidified atmosphere of free-gas exchange with change of medium every other day. Results are presented as mean ± SD of one experiment in triplicate. Lowercase letters denote significant differences according to the Student's t-test ($P \leq 0.05$).

Figure 2. Expression of stemness markers by IPI-SA3-C4 cells. The expression of stemness markers by IPI-SA3-C4 cells at indicated passages was evaluated in proliferating (P) and quiescent (Q) cells by RT-PCR using specific primers for each gen. *GAPDH* was used as positive control and RT^- as negative control (**2A**). IPI-SA3-C4 cells from 19th and 24th passages were stained with the POU5F1 (**2B**) and SOX2 (**2C**) antibodies. At least 300 cells per preparation were counted (**2D**). Results are presented as mean ± SD.

Figure 3. Karyotype and tumorigenesis analysis of IPI-SA3-C4 cells. A. The karyotype of IPI-SA3-C4 at the 20th passage. Giemsa-stained chromosomes sorted according to their size and centromere position. B. Soft-agar colony formation assay. HeLa and IPI-SA3-C4 cells (II, IV) were grown in polystyrene plates or in anchorage independently for 14 days. C. *In vivo* tumorigenesis assay in

nude mice. HeLa (I) and IPI-SA3-C4 cells (II) we implanted and tumors were left to grow for 14 days. Representative images of both experiment groups are shown, arrows illustrate the injection sites.

Figure 4. **Adipogenic capacity of IPI-SA3-C4 cells at early and late passages.** Total RNA from exponentially growing (P), quiescent non-induced (Q), freshly adipose-induced (I) and terminally adipose-differentiated (A) IPI-SA3-C4 cells at the15th and 23rd passages was analyzed by RT-PCR using specific primers for the indicated adipose markers. *GAPDH* was used as positive and RT^{-} as negative controls (**4A**). Quiescent non-adipose-induced (**4Ba, 4Bb**) and terminally adipose differentiated (**4Bc, 4Bd**) IPI-SA3-C4 cells in the 15th passage were stained with Nile Red and 4',6-diamidino-2-phenylindole (DAPI) (**4Bb 4Bd**). The formation of adipose clusters and fluorescence Red Nile/DAPI rates (**4C**), GPDH activity (**4D**) and 2-NBDG uptake (**4E**) of IPI-SA3-C4 cells under basal or stimulated conditions were also evaluated for cell populations at the indicated passages as described in Methods. Results are presented as mean ± SD of typical experiments in triplicate. Lowercase letters denote significant differences according to the Student's *t*-test ($p \leq 0.05$).

Figure 5. **Osteogenic capacity of IPI-SA3-C4 cells at early and late passages.** Total RNA from exponentially growing (P), quiescent non-induced (Q) and mature osteoblast (MO) IPI-SA3-C4 cells at the 15th and 23rd passages was analyzed by RT-PCR using specific primers for the indicated osteogenic markers. *GAPDH* was used as positive and RT^{-} as negative controls (**5A**). Quiescent non-induced (**5Ba, 5Bc, 5Be, 5Bg**) and osteogenic-induced (**5Bb, 5Bd, 5Bf, 5Bh**) IPI-SA3-C4 cells from the indicated passages were stained with leukocyte alkaline phosphatase kit (**5Ba-5Bd**) or Alizarin red (**5Be-5Bh**). The alkaline phosphatase activity (**5C**) and Alizarin red staining (**5D**) of IPI-SA3-C4 cells under basal or stimulated conditions were quantified at the indicated passages as is indicated in Methods. Quiescent human dermal fibroblasts (HDF) were used as negative control. Results are

presented as mean ± SD of one experiment in triplicate. Lowercase letters indicate significant differences according to the Student's *t*-test ($p \leq 0.05$).

Figure 6. **Chondrogenic capacity of IPI-SA3-C4 cells at early and late passages.** Total RNA from quiescent, non-induced in monolayer culture (Q), micromass in basal medium (BM) and micromass in chondrogenic medium (CM) IPI-SA3-C4 cells at the15th and 23rd passages was analyzed by RT-PCR using specific primers for the indicated chondrogenic and osteogenic markers. *GAPDH* was used as positive and RT^{-} as negative controls (**6A**). Micrographs of IPI-SA3-C4 micromasses were taken under fixed (Phase-contrast) and Alcian Blue stained cultures (**6B**). Micromass diameters were determinate from micrographs at 1st and 21st days of culture (**6C**). Results are presented as mean ± SD of one experiment in triplicate. Lowercase letters significant differences according to the Student's *t*-test ($p \leq 0.05$).

5.2. Rapid expansion and transient hTERT activity of IPI-SA3-C4 strain by the optimization of its culture conditions

The IPI-SA3-C4 cells possess a high proliferative capacity, however as shown in the first part of the results, these cells have a lifespan limited. Here, we searched to circumvent this drawback by attempting its establishment as an immortalized cell line. To reach this goal, we carried out several experiments, which included the ectopic overexpression of hTERT or/and SV40gp6 sequences by the use of retroviral or episomal vectors. The use of retroviral vectors included the transduction/infection of IPI-SA3-C4 cells with viral particles. In spite of accomplishing the optimization of transfection techniques, we only achieved a 10% of transfected cells as the highest proportion after a series of different trials. Such low percentage of transfected cells in addition to the low probability to obtain a cell population with the ability to surpass the M1 and M2 stages of the crisis of the cell population, did not allow to cope the limited life-span of IPI-SA3-C4 cells. After transfection, the IPI-SA3-C4 cells entered in growth arrest, independently of the strength of the promoter used for the overexpression of hTERT or/and SV40gp6. We must remark that in our experiments we used CMV and EF-1α promoters, and we obtained similar final results, leading to give up the application of this strategy on IPI-SA3-C4 cells. In a comparative study, Maurisse et al., 2010 showed that some cells are easier to transfect than others, using same or different transfection protocols. In such experiments they found that primary human airway epithelial cells were difficult to transfect. Currently, the explanation for these results is still uncertain (Murisse, et al., 2010).

Alternatively, we attempted to cope the limited life-span of IPI-SA3-C4 cells by the use of conditioned-culture medium by human embryonic stem cells (CM), and a combination of conditioned medium-extracellular matrix (EM). In preliminary experiments, assays using L15-medium, mTeSR1, and CM, Polyestyrene (P), Matrigel (M) and EM, resulted in enhanced proliferation of IPI-SA3-C4 cells, since the doubling time was decreased, and the saturation cell density was increased. Thus, 50% dilutions of mTeSR1 decreased the duplication time of IPI-SA3-C4 cells by 28% and increased the saturation density by 585% when compared to control condition P.L15 (Fig. 1A, 1B). Subsequently, based on these results, we choose the optimal culture conditions for the long-term growth IPI-SA3-C4 cells *in vitro.* In these experiments cells were subcultured serially every 3 days, and were plated at the same cell density, being supplemented either with P.L15 + mTesR1 50%; or M.L15 + mTesR1 50% to compare life-span of the cells under such culture conditions. When cells were cultured under control conditions (P.L15), their lifespan achieved ~63 population doublings (PDLs). In contrast, the use of the 50% mTeSR1 dilution as supplementation for cell cultures resulted in a significant increment of PDL number for cultivation onto polystyrene (76 PDLs) and Matrigel (74 PDLs) (Fig.1C). We also tested the effect of L15-mTeSR1 on the colony-forming efficiency of IPI-SA3-C4 cells. IPI-SA3-C4 cells showed in control conditions a clonal efficiency of 13%, whereas growth in L15-mTESR1, the colony forming efficiency increased by 29% on uncoated and 28% on Matrigel®-coated dishes. Cells at the 12th passage were unable to form colonies under control culture conditions and when they were grown in L15-mTESR1 showed minimal clonal efficiencies (1% uncoated and 2% Matrigel®-coated dishes) (Fig. 1D).

Moreover, as chromosomal rearrangements may occur during prolonged cultivation we karyotyped IPI-SA3-C4 cells grown for 10 passages in L15-mTESR1 and uncoated or Matrigel®-coated dishes. No chromosome number alterations and larger chromosome defects were found in any of the studied karyotypes (Fig. 1E). Surprisingly, the adipogenic potential of IPI-SA3-C4 cells was maintained, because similar rates of intracytoplasmic lipid accumulation were found as judged by Nile red staining (Fig. 2A–B). As in the case of cell growth, the presence of Matrigel® as culture substrate did not increase the adipogenic potential. Furthermore, the expression of adipogenic markers *CEBPB*, *CEBPD*, *PPARG* and *LEP* was increased significantly when L15-mTeSR1 was used for cultivation at both passages 4 and 8, with the exception of *LEP* for passage 8 cells (Fig. 2C–F).The expression of stemness markers *POU5F1 (OCT4)*, *SOX2*, *NANOG*, *MYC*, and *hTERT* is associated with pluripotency and self-renewal. The mRNAs for *OCT4*, *SOX2*, *MYC* and *hTERT*, but not that of *NANOG*, were upregulated to a variable degree in cells grown in modified growth conditions (Fig. 3A–E). Notably, the expression of *hTERT* mRNA was drastically increased in cells cultivated in L15-mTeSR1 regardless of dish coating correlating well with their increased growth potential (Fig. 3E). Moreover, when hTERT was observed in immunofluorescence experiments, we could detect it in the nucleus of IPI-SA3-C4 cells grown under all cell culture conditions tested, however, its cytoplasmic location was observed only in cells grown with mTeSR1 at 50% (Fig. 4A). Accordingly, the percentage of cells with nuclear and cytoplasmic hTERT was highest in cells grown in L15-mTeSR1on uncoated (47.5% and 45.2% respectively) and on Matrigel®-coated (33.78% and 10.13% respectively) dishes than in the control cells (28.26% and 0.93%

Figure 1. Growth and karyotype analysis of IPI-SA3-C4 cells under diverse culture conditions.

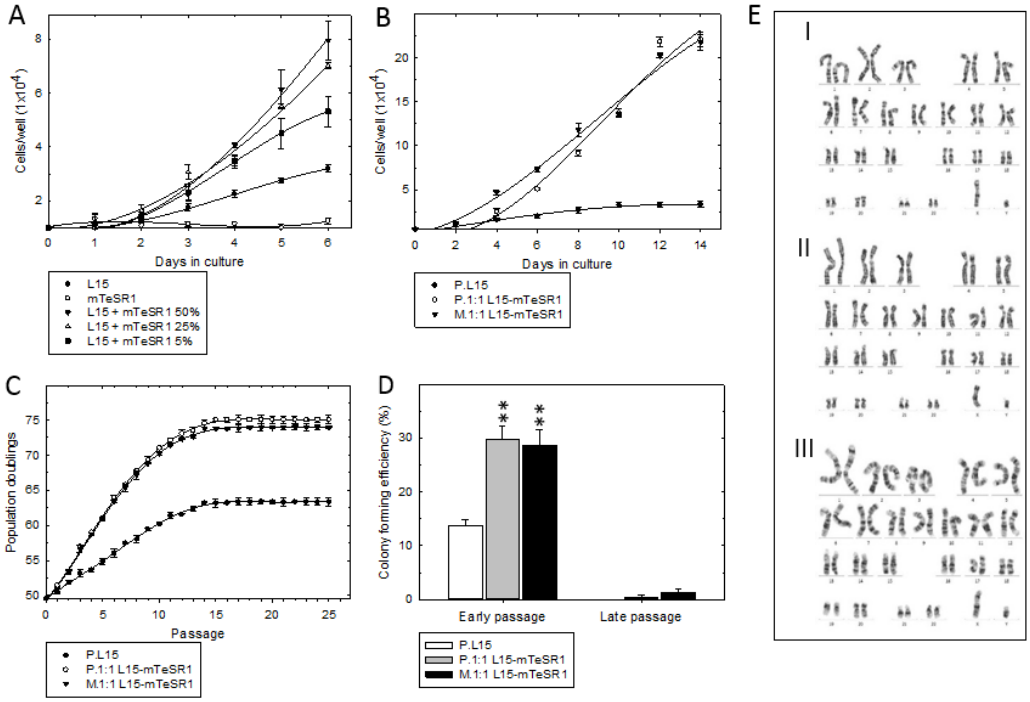

Figure 2. Adipogenic differentiation potential of IPI-SA3-C4 cells grown under modified growth conditions.

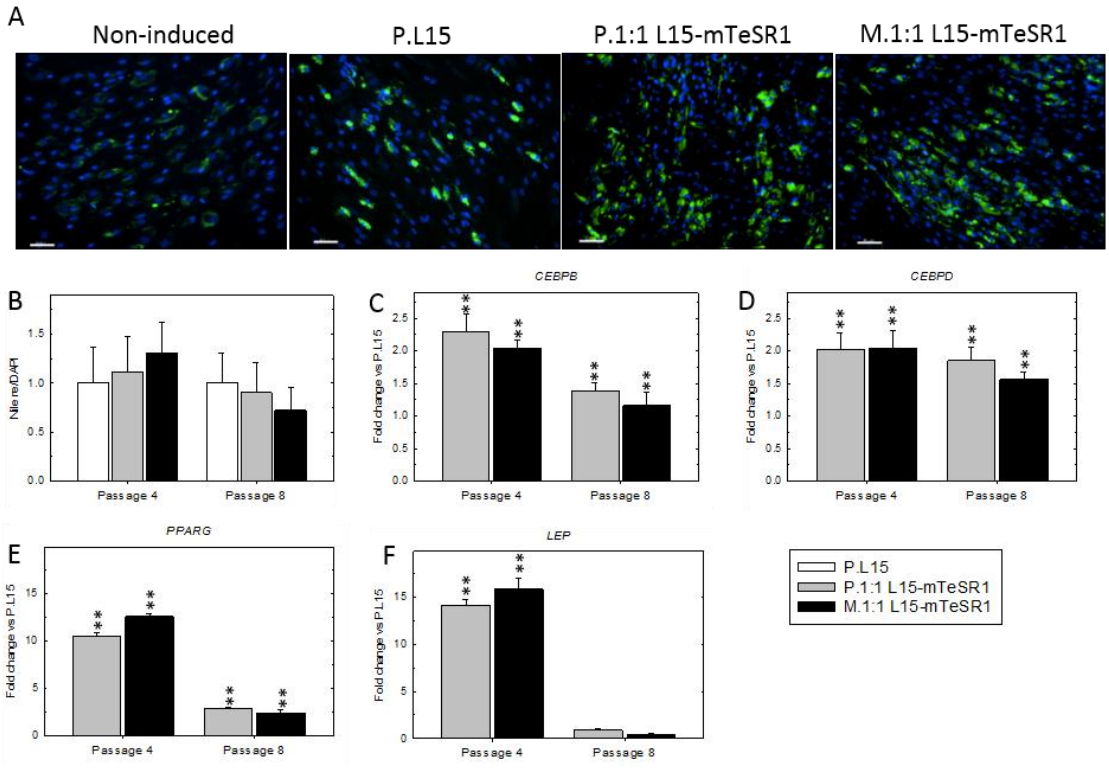

Figure 3. Expression of stemness genes in IPI-SA3-C4 cells.

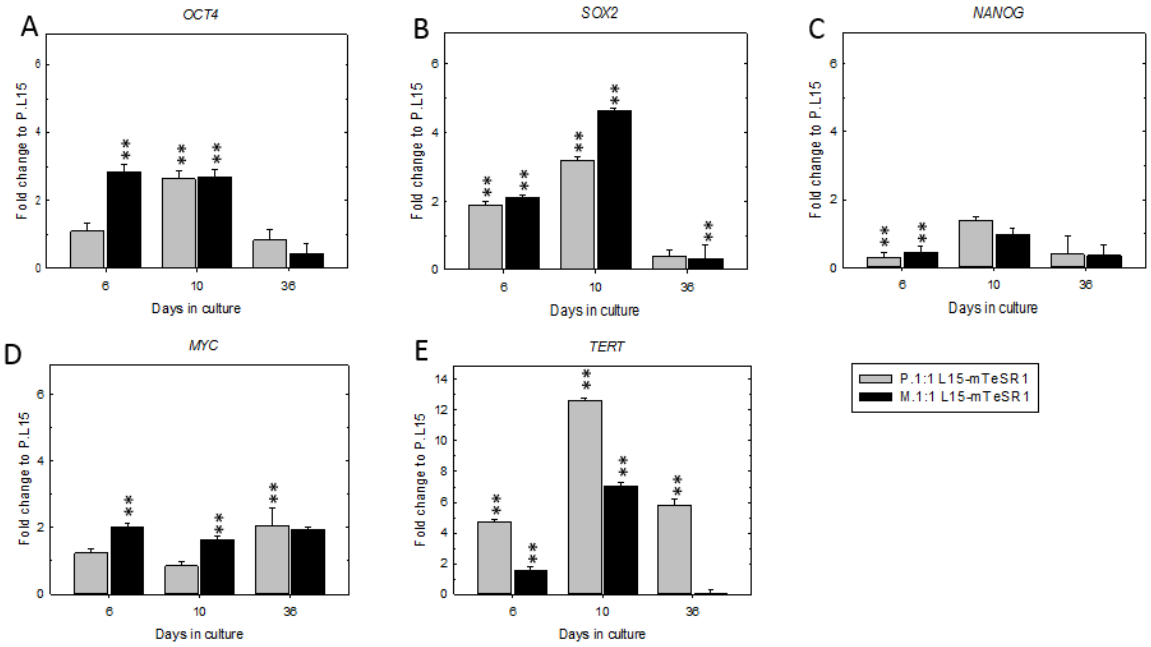

Figure 4. Presence of TERT, its inhibition, and telomere length in IPI-SA3-C4 cells.

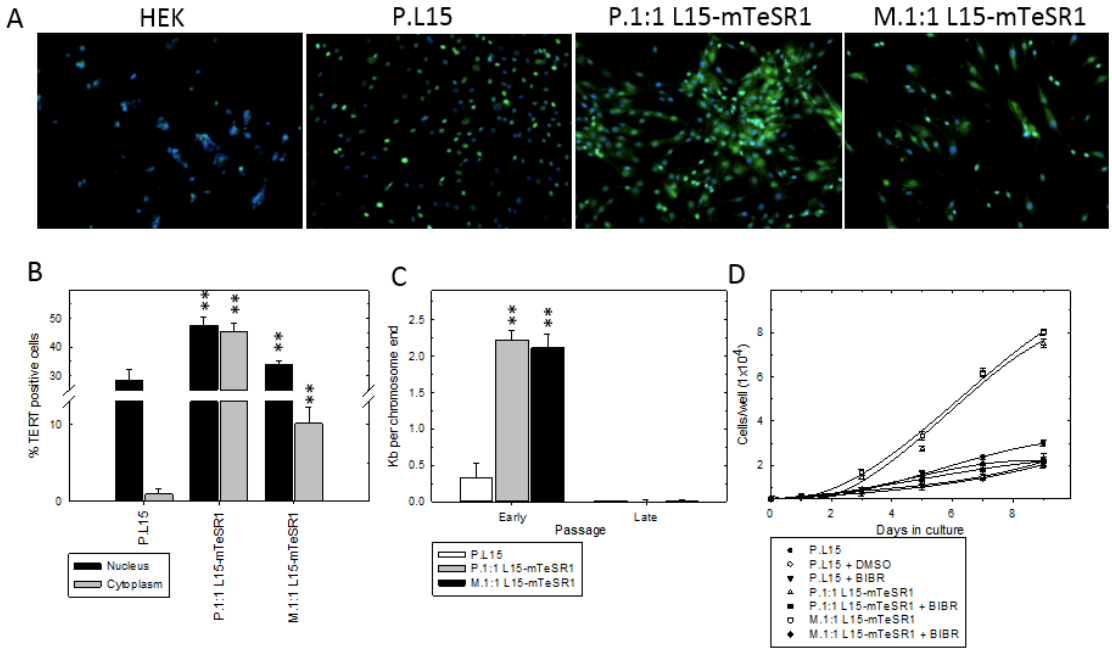

respectively) (Fig. 4B). Furthermore, the indirect activation of the protein was confirmed by measuring the telomere length of the cells grown under the different treatments, and as expected, the longest telomeres were found in cells grown in 50% mTeSR1were at least 6.39 times longer than cells cultured in L15at early passage (Fig. 4C). Finally, in an assay using a specific hTERT inhibitor, we demonstrated the direct effect of hTERT activity on proliferative capacity of IPI-SA3-C4 cells with mTeSR1 50% dilutions (Fig. 4D). While searching for the potential mechanism of mTeSR1-induced increase in proliferative capacity we noted that the increased expression of *hTERT* mRNA and accumulation of nuclear and cytoplasmic hTERT protein during the early cell passages correlated with higher PD numbers of cells cultivated in L15-mTeSR1. Cytoplasmic hTERT has been shown to enhance cell survival by reducing stress in endoplasmic reticulum, lysosomes and Golgi apparatus and by protecting mitochondrial integrity (Zhou et al., 2014; Chiodi et al., 2012; El-Hafeez 2018). Nuclear hTERT is necessary for maintenance of the telomere integrity and in concordance with this we found that in early cultures grown in L15-mTeSR1 the telomeres were longer than in case of other growth conditions. In aging cultures length of the telomeres was equally shortened indicating that additional mechanisms apart from hTERT activity control the life span of the cultured primary cells. The importance of hTERT activity in regulating the multiplication capacity of IPI-SA3-C4 cells was underlined by the reduction of proliferative activity to the control level when an hTERT inhibitor was added to the cultures grown in L15-mTeSR1. mTeSR1 contains high concentration of fibroblast growth factor 2 (FGF-2) (100 ng/ml) (Zou et al., 2017). Diverse studies have showed that in addition to hESC FGF-2 enhances the proliferation of human

cells with diverse tissue origin (Hebert et al., 2009; Zaragosi et al., 2006; Bianchi et al., 2003). In addition to exogenous FGF2 the production of endogenous FGF2 by hADSCs is the key factor for long-term propagation and self-renewal (Zaragosi et al., 2006; Rider et al., 2008]). The signaling pathway from FGF2 to hTERT is not clear yet. FGF2 can upregulate WNT3A and WNT5A expression in synovium-derived stem cells (Kakudo et al., 2019; Pizzute et al., 2016) and it has been proposed that FGF-2 upregulates hTERT expression and telomerase activity via Wnt/β-catenin signaling pathway in hESC (Zou et al., 2017). It is worth noting that in previous studies utilizing non-embryonic cells the FGF-2 concentrations in growth media have been 20 ng/ml or below. In our experiments the final FGF-2 concentration was 50 ng/ml in L15-mTeSR1. Thus, here we show for the first time the effects of high concentration of FGF in human primary preadipocytes.

5.2.1 Figure legends

Figure 1. Growth and karyotype analysis of IPI-SA3-C4 cells under diverse culture conditions. **A**. Kinetic under mTeSR1 dilutions. **B**. Kinetic under L15-mTeSR1. **C**. Population doublings (PD) during long term growth. **D**. Colony-forming assay. **E.** Karyotyping of passage 10 IPI-SA3-C4 cells. I. P.L15; II. P. L15-mTeSR1; III. M. L15-mTeSR1. P - Polystyrene dishes, M - Matrigel®-coated dishes. Results are presented as mean ± SD. ** $P < 0.01$.

Figure 2. Adipogenic differentiation potential of IPI-SA3-C4 cells grown under modified growth conditions. **A**. Nile red staining of non-induced and induced IPI-SA3-C4 cells. **B**. Quantification of Nile red signal. The expression levels of *CEBPB* (**C**), *CEBPD* (**D**), *PPARG* (**E**), and *LEP* (**F**) mRNA. Results are presented as mean ± SD. ** $P < 0.01$.

Figure 3. Expression of stemness genes in IPI-SA3-C4 cells. The expression level of *OCT4* **(A**), *SOX2* **(B)**, *NANOG* **(C)**, *MYC* (**D)** and *hTERT* (**E)** mRNA. Results are presented as mean ± SD. ** $P < 0.01$.

Figure 4. Presence of TERT, its inhibition, and telomere length in IPI-SA3-C4 cells. **A**. Immunofluorescence analysis of hTERT **B**. Quantification of hTERT expression. **C**. Evaluation of telomere lengths in early (1st) and late (20th) passages IPI-SA3-C4 cells. **D**. Effects to growth IPI-SA3-C4 cells with hTERT inhibitor (BIBR) in L15-mTeSR1. Results are presented as mean ± SD; ** $P < 0.01$.

6. Conclusions

Our results show that the IPI-SA3-C4 cells are a clonal population of normal human diploid subcutaneous mesenchymal cells with high proliferative capacity that supports prolonged passaging in culture. IPI-SA3-C4 cells could be an *in vitro* model system suitable to study human adipogenesis. The use of 50% mTeSR1 medium dilution in L15 medium allows extend approximately 20% the life-span of the IPI-SA3-C4 cells, which is a novel and alternative method to enhance the proliferative properties. Moreover, under these culture conditions the adipogenic differentiation capacity is maintained without cell karyotype changes. This effect is mediated at least in part by an increase in hTERT activity yielding a potent tool for further studies of human adipogenesis *in vitro*.

7. References

1. González-Casanova JE, Pertuz-Cruz SL, Caicedo-Ortega NH, et al, 2020. Adipogenesis regulation and endocrine disruptors: Emerging insights in obesity. Biomed Res Int, https://doi.org/10.1155/2020/7453786.
2. Chait A, Hartigh J den, 2020.Adipose tissue distribution, inflammation and its metabolic consequences, including diabetes and cardiovascular disease. Front Cardiovasc Med, 7:22.
3. Aragonès G, Ardid-Ruiz A, Ibars M, et al, 2016. Modulation of leptin resistance by food compounds. Mol Nutr Food Res, 60:1789–803.
4. Catteau A, Caillon H, Barrière P, Denis MG, Masson D, Fréour T, 2016. Leptin and its potential interest in assisted reproduction cycles. Hum Reprod Update, 22:320–341.
5. Armani A, Mammi C, Marzolla V, et al, 2010. Cellular models for understanding adipogenesis, adipose dysfunction, and obesity. J Cell Biochem, 110:564–72.
6. Ruiz-Ojeda FJ, Rupérez AI, Gomez-Llorente C, et al, 2016. Cell models and their application for studying adipogenic differentiation in relation to obesity: A review. Int J Mol Sci, 17, 1040.
7. Cristancho AG, Lazar MA, 2011. Forming functional fat: a growing understanding of adipocyte differentiation. Nature, 12:722–734.
8. Jozefczuk J, Drews K, Adjaye J, 2012. Preparation of mouse embryonic fibroblast cells suitable for culturing human embryonic and induced pluripotent stem cells. J Vis Exp, e3854 10.3791/3854.
9. Church C, Brown M, Rodeheffer MS, 2014. Conditional immortalization of primary adipocyte precursor cells. Adipocyte, 0:1–9.
10. Zuk PA, Zhu M, Mizuno H, et al, 2001. Multilineage cells from human adipose tissue: implications for cell-based therapies. Tissue Eng, 7:211–228.
11. Cawthorn WP, Scheller EL, MacDougald OA, 2012. Adipose tissue stem cells meet preadipocyte commitment: going back to the future. J Lipid Res, 53:227–246.

12. Heo JS, Choi Y, Kim HS, 2016. Comparison of molecular profiles of human mesenchymal stem cells derived from bone marrow, umbilical cord blood, placenta and adipose tissue. Int J Mol Med, 37:115–125.
13. Viswanathan S, Shi Y, Galipeau J, et al, 2019. Mesenchymal stem versus stromal cells: International Society for Cellular Therapy Mesenchymal Stromal Cell committee position statement on nomenclature. Cytotherapy. 00:1–6.
14. Guasti L, New SE, Hadjidemetriou I, et al, 2018. Plasticity of human adipose-derived stem cells – relevance to tissue repair. Int J Dev Biol, 62:431–439.
15. Sikora E, Bielak-zmijewska A, Mosieniak G, 2018. What is and what is not cell senescence. Postępy Biochemii, 64:2-3.
16. Hayflick L, 1965. The limited in vitro lifetime of human diploid cell strains. Exp Cell Res, 636:614–36.
17. Bond JA, Haughton MF, Rowson JM, et al, 1999. Control of replicative life span in human cell: Barriers to clonal expansion intermediate between M1 senescence and M2 crisis. Mol Cell Biol, p.3101-31114.
18. Fridman AL, Tainsky MA, 2008. Critical pathways in cellular senescence and immortalization revealed by gene expression profiling. Oncogene, 9;27(46).
19. Freshney RI. Culture of animal cells. Cytotoxicity 2010.
20. Conese M, Auriche C, Ascenzioni F, 2004. Gene therapy progress and prospects: Episomally maintained self-replicating systems. Gene therapy, 11:1735-1741.
21. Todaro GJ, Green H, 1963. Quantitative studies of the growth of mouse embryo cells in culture and their development into established lines. J Cell Biol, 17:299–313.
22. Lo HL, Yee JK, 2007. Production of vesicular stomatitis virus G glycoprotein (VSV-G) pseudotyped retroviral vectors. Curr Protoc Hum Genet, Chapter 12:Unit 12.7.
23. Balducci L, Blasi A, Saldarelli M, et al, 2014. Immortalization of human adipose-derived stromal cells: production of cell lines with high growth rate, mesenchymal marker expression and capability to secrete high levels of angiogenic factors. Stem Cell Res Ther**,** 5:63.

24. Drayman N, Ben-nun-shaul O, Butin-israeli V, et al, 2016. p53 elevation in human cells halt SV40 infection by inhibiting T-ag expression. Oncotarget, 7:52643-52660.
25. Takeuchi M, Takeuchi K, Kohara A, et al, 2007. Chromosomal instability in human mesenchymal stem cells immortalized with human papilloma virus E6, E7, and hTERT genes. In Vitro Cell Dev Biol Anim, 43:129–38.
26. Kelekar A, Cole M D, 1987. Immortalization by c-myc, H-ras, and E1a oncogenes induces differential cellular gene expression and growth factor responses. Mol Cell Biol. 7:3899–3907.
27. Darimont C, Zbinden I, Avanti O, et al, 2003. Reconstitution of telomerase activity combined with HPV-E7 expression allow human preadipocytes to preserve their differentiation capacity after immortalization. Cell Death Differ, 10:1025–31.
28. Jiang L, Li J, Song L, 2009. Bmi-1, stem cells and cancer. Acta Biochim Biophy Sin, 41:527-534.
29. Rosler ES, Fisk GJ, Ares X, et al, 2004. Long-Term Culture of Human Embryonic Stem Cells in Feeder-Free Conditions. Dev Dyn, 229:259–74.
30. Mathew R, Jia W, Sharma A, et al, 2010. Robust activation of the human but not mouse telomerase gene during the induction of pluripotency. FASEB J, 24:2702–2715.
31. Takahashi K, Yamanaka S, 2006. Induction of pluripotent stem cells from mouse embryonic and adult fibroblast cultures by defined factors. Cell, 126:663–676.
32. Csobonyeiova M, Polak S, Koller J, et al 2015. Induced pluripotent stem cells and their implication for regenerative medicine. Cell Tissue Bank, 16:171–180.
33. Liu P, Chen M, Liu Y, et al, 2018. CRISPR-Based Chromatin Remodeling of the Endogenous Oct4 or Sox2 Locus Enables Reprogramming to Pluripotency. Cell Stem Cell, 22:252–261.
34. Diecke S, Lu J, Lee J, et al 2015. Novel codon-optimized mini-intronic plasmid for efficient, inexpensive, and xeno-free induction of pluripotency. Sci Rep, 5:8081.

35. Peng R, Lin G, Li J, 2016. Potential pitfalls of CRISPR/Cas9-mediated genome editing. FEBS J, 283:1218–31.
36. Haendeler J, Hoffmann J, Diehl JF, et al, 2004. Antioxidants inhibit nuclear export of telomerase reverse transcriptase and delay replicative senescence of endothelial cells. Circ Res, 94:768–75.
37. Choi H, Cho K, Kang H, et al, 2011. Restoration of senescent human diploid fibroblasts by modulation of the extracellular matrix. Aging Cell, 10:148–57.
38. Prasajak P, Rattananinsruang P, Chotinantakul K, et al, 2015. Embryonic stem cells conditioned medium enhances Wharton's jelly-derived mesenchymal stem cells expansion under hypoxic condition. Cytotechnology, 6:493–505.
39. Paula ACC, Martins TMM, Zonari A, et al, 2015. Human adipose tissue-derived stem cells cultured in xeno-free culture condition enhance c-MYC expression increasing proliferation but bypassing spontaneous cell transformation. Stem Cell Res Ther, 6:76.
40. Conboy IM, Conboy MJ, Wagers AJ, et al, 2005. Rejuvenation of aged progenitor cells by exposure to a young systemic environment. Nature, 433:760–4.
41. Vatolin S, Radivoyevitch T, Maciejewski JP, 2019. New drugs for pharmacological extension of replicative life span in normal and progeroid cells. NPJ Aging Mech Dis, doi: 10.1038/s41514-018-0032-4.
42. Green H, Kehinde O, 1975. An established preadipose cell line and its differentiation in culture II. Factors affecting the adipose conversion. Cell, 5:19–27.
43. Green H, Kehinde O, 1976. Spontaneous heritable changes leading to increased adipose conversion in 3T3 cells. Cell, 7:105–113.
44. Wabitsch M, Brenner RE, Melzner I, et al, 2001. Characterization of a human preadipocyte cell strain with high capacity for adipose differentiation. Int J Obes, 25:8–15.
45. Lane MD, Tang Q, Jiang M, 1999. Role of the CCAAT enhancer binding proteins (CEBPs) in adipocyte differentiation. Biochem Bioph Res Co, 266:677–683.

46. Mikkelsen TS, Xu Z, Zhang X, et al, 2010. Comparative epigenomic analysis of murine and human adipogenesis. Cell, 143:156-169.
47. Morrison S, McGee SL, 2015. 3T3-L1 adipocytes display phenotypic characteristics of multiple adipocyte lineages. Adipocyte, 3945:295–302.
48. Yeo CR, Agrawal M, Hoon S, et al, 2017. SGBS cells as a model of human adipocyte browning: A comprehensive comparative study with primary human white subcutaneous adipocytes. Sci Rep 7:4031
49. Montanari T, Colitti M, 2018. Simpson-Golabi-Behmel syndrome human adipocytes reveal a changing phenotype throughout differentiation. Histoch Cell Biol, 149:593-605.
50. Okamoto T, Aoyama T, Nakayama T, et al 2002. Clonal heterogeneity in differentiation potential of immortalized human mesenchymal stem cells. Biochem Bioph Res Co, 295:354–361.
51. Wolbank S, Stadler G, Peterbauer A, et al, 2009. Telomerase immortalized human amnion- and adipose-derived mesenchymal stem cells: Maintenance of differentiation and immunomodulatory characteristics. Tissue Eng Part A, 15:1843–1854.
52. Green H, Kehinde O, 1974. Sublines of mouse 3T3 cells that accumulate lipid. Cell, 1:113–116.
53. Spiegelman BM, Frank M, Green H, 1983. Molecular cloning of mRNA from 3T3 adipocytes. Regulation of mRNA content for glycerophosphate dehydrogenase and other differentiation-de pendent proteins during adipocyte development. J Biol Chem, 258:10083–10089.
54. Wolins NE, Quaynor BK, Skinner JR, et al, 2005. OP9 mouse stromal cells rapidly differentiate into adipocytes: characterization of a useful new model of Adipogenesis. J Lipid Res, 47:450-460.
55. Aaronson SA, Todaro GJ, 1968. Development of 3T3-like lines from Balb/c mouse embryo cultures: Transformation susceptibility to SV40. J Cell Physiol 72:141–148.
56. Gharbi-Chihi J, Grimaldi P, Torresani J, et al, 1981. Triiodothyronine and adipose conversion of OB17 preadipocytes: binding to high affinity sites and

effects on fatty acid synthesizing and esterifying enzymes. J Recept Res 2:153–173.

57. Zilberfarb V, Piétri-Rouxel F, Jockers R, et al. 1997. Human immortalized brown adipocytes express functional β3-adrenoceptor coupled to lipolysis. J Cell Science, 110:801-807.
58. Herrera-Herrera Ml, Zapata-Bustos R, Salazar-Olivo LA, 2009. Simplified culture techniques for growth and differentiation of murine and human pre-adipocytes for translational applications. Cytotherapy, 11:52–60.
59. Suga H, Shigeura T, Matsumoto D, Inoue K, Kato H, Aoi N, Murase S, Sato K, Gonda K, Koshima I, et al. 2007 Rapid expansion of human adipose-derived stromal cells preserving multipotency. Cytotherapy, 9: 738-745.
60. Böcker W, Yin Z, Drosse I, Haasters F, Rossmann O, Wierer M, Popov C, Locher M, Mutschler W, Docheva D, et al. 2008. Introducing a single-cell-derived human mesenchymal stem cell line expressing hTERT after lentiviral gene transfer. J Cell Mol Med, 12: 1347-59.
61. Alonso-Castro AJ, Zapata-Bustos R, Domínguez F, García-Carrancá A, Salazar-Olivo LA. 2011. *Magnolia dealbata* Zucc and its active principles honokiol and magnolol stimulate glucose uptake in murine and human adipocytes using the insulin-signaling pathway. Phytomedicine 18:926-933.
62. Aldridge A, Kouroupis D, Churchman S, English A, Ingham E, Jones E. 2013. Assay validation for the assessment of adipogenesis of multipotential stromal cells - a direct comparison of four different methods. Cytotherapy 15:89-101.
63. Birmingham E, Niebur GL, McHugh PE, Shaw G, Barry FP, McNamara LM. 2012. Osteogenic differentiation of mesenchymal stem cells is regulated by osteocyte and osteoblast cells in a simplified bone niche. Eur Cells Mater 23:13-27.

64. Gregory CA, Gunn WG, Peister A, Prockop DJ. 2004. An Alizarin red-based assay of mineralization by adherent cells in culture: Comparison
65. Sabokbar A, Millett PJ, Myer B, Rushton N. 1994. A rapid, quantitative assay for measuring alkaline phosphatase activity in osteoblastic cells in vitro. Bone Miner 27:57-67.
66. Ahrens PB, Solursh M, Reiter RS. 1977. Stage-related capacity for limb chondrogenesis in cell culture. Dev Biol 60:69-82.
67. Denker AE, Nicoll SB, Tuan RS. 1995. Differentiation. Formation of cartilage-like spheroids by micromass cultures of murine C3H10T1/2 cells upon treatment with transforming growth factor-β1. Differentiation 59:25-34.
68. Stultz BG, McGinnis, K, Thompson EE, Lo Surdo JL, Bauer SR, Hursh DA. 2016. Chromosomal stability of mesenchymal stromal cells during in vitro culture Cytotherapy 18:336-343.
69. Borowicz S, Van Scoyk M, Avasarala S, Rathinam MKK, Tauler J, Bikkavilli RK, Winn RA. 2014. The soft agar colony formation assay. J Vis Exp 92:e51998.
70. M. Klaas, K. Mäemets-Allas, K. Lõhmussaar, et al. 2019. Endogenous beta-galactosidase activity marks a TREM2-expressing Kupffer cell population in injured livers of Lgr5-LacZ and wild-type mice. FEBS Lett. doi: 10.1002/1873-3468.13669.
71. Trivanović D, Jauković A, Popović B, et al. 2015. Mesenchymal stem cells of different origin: Comparative evaluation of proliferative capacity, telomere length and pluripotency marker expression. Life Sci, 141:61–73.

72. Maurisse R, De Semir D, Emamekhoo H, et al. 2010. Comparative transfection of DNA into primary and transformed mammalian cells from different lineages. BMC Biotechnol, doi: 10.1186/1472-6750-10-9.
73. Zhou J, Mao B, Zhou Q, et al. 2014. Endoplasmic reticulum stress activate telomerase, Aging Cell, doi:10.1111/acel.12161.
74. Chiodi I, Mondello C. 2012. Telomere-independent functions of telomerase in nuclei, cytoplasm, and mitocondria, Front. Oncol, doi:10.3389/ fonc.2012.00133.
75. El-Hafeez AAA, Hosoi T, Nakatsu K, et al. 2018. TERT enhances the survival rate of human fibroblasts under endoplasmic reticulum, Golgi apparatus, and lysosomal stresses, Biotechnol. Lett. 40: 915–922.
76. Zou, H J Tong, M Li, et al. 2017. Telomere length is regulated by FGF-2 in human embryonic stem cells and affects the life span of its differentiated progenies, Biogerentology 18:69–84.
77. Hebert TL, Wu X, Yu G, et al. 2009. Culture effects of epidermal growth factor (EGF) and basic fibroblast growth factor (bFGF) on cryopreserved human adipose-derived stromal/stem cell proliferation and adipogenesis, J. Tissue Eng. Regen. Med. 3:553–561.
78. Zaragosi LE, Ailhaud G, Dani C. 2006. Autocrine fibroblast growth factor 2 signaling is critical for self-renewal of human multipotent adipose-derived stem cells, Stem Cell. 24:2412–2419.
79. Bianchi G, Banfi A, Mastrogiacomo M, et al. 2003. Ex vivo enrichment of mesenchymal cell progenitors by fibroblast growth factor 2, Exp. Cell Res. 287:98–105.
80. Rider DA, Dombrowski C, Sawyer AA, et al. 2008. Autocrine fibroblast growth factor 2 increases the multipotentiality of human adipose-derived mesenchymal stem cells, Stem Cell. 26:1598–1608.
81. Ma Y, Kakudo N, Morimoto N, et al. 2019. Fibroblast growth factor-2 stimulates proliferation of human adipose-derived stem cells via Scr activation, Stem Cell Res. Ther. 10:350.

82. Pizzute T, Li J, Zhang Y, et al. 2016. Fibroblast growth factor ligand dependent proliferation and chondrogenic differentiation of synovium-derived stem cells and concomitant adaptation of Wnt/Mitogen-Activated protein kinase signals, Tissue Eng. 22:1036–1046.

8. Published articles

A human preadipocyte cell strain with multipotent differentiation capability as an *in vitro* model for adipogenesis.

In Vitro Cellular & Developmental Biology - Animal

http://link.springer.com/article/10.1007/s11626-020-00468-z

In Vitro Cellular & Developmental Biology - Animal
https://doi.org/10.1007/s11626-020-00468-z

A human preadipocyte cell strain with multipotent differentiation capability as an in vitro model for adipogenesis

Claudia G. Cárdenas-León[1] · Angélica Montoya-Contreras[1] · Kristina Mäemets-Allas[2] · Viljar Jaks[2] · Luis A. Salazar-Olivo[1]

Received: 25 November 2019 / Accepted: 14 May 2020 / Editor: Tetsuji Okamoto

Abstract
Murine 3T3 cell lines constitute a standard model system for in vitro study of mammalian adipogenesis although they do not faithfully reflect the biology of the human adipose cells. Several human adipose cell lines and strains have been used to recapitulate human adipogenesis in vitro, but to date there is no generally accepted in vitro model for human adipogenesis. We obtained a clonal strain of human subcutaneous adipose stromal cells, IPI-SA3-C4, and characterized its utility as an in vitro model for human subcutaneous adipogenesis. IPI-SA3-C4 cells showed a high proliferative potential for at least 30 serial passages, reached 70 cumulative population doublings and exhibited a population doubling time of 47 h and colony forming efficiency of 12% at the 57th cumulative population doublings. IPI-SA3-C4 cells remained diploid (46XY) even at the 56th cumulative population doublings and expressed the pluripotency markers *POU5F1*, *NANOG*, *KLF4*, and *MYC* even at 50th

Keywords Human subcutaneous preadipocytes · Cellular model · Adipogenesis · Osteogenesis · Chondrogenesis

Introduction

Mammalian white adipose tissue serves as the main triglyceride accumulation depot that functions as an energy reservoir set aside for periods of food shortage (Peirce et al. 2014; Zwick et al. 2018). White adipose tissue acts also as an endocrine organ producing adipokines that connect metabolism with immune system (Heo et al. 2016; Francisco et al. 2018) and is an optimal source of multipotent adult stem cells. Thus, studying white adipose tissue will increase our knowledge on the mechanisms underlying obesity and diabetes, two worldwide diseases that account for a huge burden on the healthcare system (Cho et al. 2018; Francisco et al. 2018), and would expand our proficiency in using these cells in regenerative medicine (Heo et al. 2016).

Multiple aspects of adipose tissue biology can be addressed using in vitro experimental models such as preadipocyte primary cultures and established preadipose cell lines. Preadipocyte primary cultures show high similarity to normal adipocytes in vivo and usually remain euploid. However, such primary cells have a limited lifespan in vitro and their adipogenic capacity gradually decreases during ex vivo cultivation (Hayflick 1965). On the other hand, established preadipose cell lines have unlimited proliferative capacity, but do not show all the functional characteristics of normal adipose cells (Freshney 2010).

Diverse cell lines have been utilized as in vitro experimental model of adipose tissue. Although the murine 3T3 cell lines (Green and Kehinde 1975, 1976) and the human cells SGBS (Wabitsch et al. 2001) and Chub-S7 (Darimont et al. 2003) have extensively been used for modeling different aspects of the adipose tissue biology, several lines of evidence show their use as full-featured human adipose tissue models is rather limited. For example, 3T3-L1 and 3T3-F442A are aneuploid embryonal cells of unknown tissue origin; they display

✉ Luis A. Salazar-Olivo
olivo@ipicyt.edu.mx

[1] División de Biología Molecular, Instituto Potosino de Investigación Científica y Tecnológica, Camino a la Presa San José 2055, 78216 San Luis Potosí, SLP, Mexico

[2] Department of Cell Biology, Institute of Molecular and Cell Biology, University of Tartu, Tartu, Estonia

Published online: 13 June 2020

Enhanced proliferative capacity of human preadipocyte achieved by an optimized cultivating method that induces transient activity of hTERT

Biochemical and Biophysical Research Communications. In press.

Contents lists available at ScienceDirect

Biochemical and Biophysical Research Communications

journal homepage: http://ees.elsevier.com

Enhanced proliferative capacity of human preadipocytes achieved by an optimized cultivating method that induces transient activity of hTERT

Claudia G. Cárdenas-León[a], Kristina Mäemets-Allas[b], Kati Kuuse[c], Luis A. Salazar-Olivo[a], Viljar Jaks[b,d,*]

[a] División de Biología Molecular, Instituto Potosino de Investigación Científica y Tecnológica, San Luis Potosí, Mexico
[b] Department of Cell Biology, Institute of Molecular and Cell Biology, University of Tartu, Estonia
[c] Department of Clinical Genetics, United Laboratories, Tartu University Hospital, Tartu, Estonia
[d] Dermatology Clinic, Tartu University Hospital, Tartu, Estonia

ARTICLE INFO

Article history:
Received 29 April 2020
Accepted 4 June 2020
Available online xxx

Keywords
Adipose-derived stromal cells
mTesR1
Adipogenesis
hTERT
Senescence

ABSTRACT

Human mesenchymal stromal cells (MSC) are an important tool for basic and translational research. Large amounts of MSC are required for *in vitro* and *in vivo* studies, however, the limited life-span and differentiation ability *in vitro* hamper their optimal use. Here we report that 1:1 mixture of L15 and mTeSR1 culture media increased the life-span of IPI-SA3-C4, a normal non-immortalized human subcutaneous preadipocyte strain by 20% while retaining their adipogenic capacity and stable karyotype. The increased proliferative capacity was accompanied by increased expression of the stem markers *POU5F1*, *SOX2*, *MYC* and *hTERT*, and inhibition of hTERT activity abolished the growth advantage of L15-mTeSR1. Consequently, the described MSC culture would considerably enhance the utility of MSC for *in vitro* studies.

1. Introduction

Human mesenchymal stromal cells (MSC) are self-renewable cells that possess the capacity to differentiate into adipocytes, osteoblasts and chondrocytes, and present a specific surface marker profile [1]. Numerous studies have revealed clinically important properties of MSC such as immunomodulatory [2], neurotrophic [3], anti-microbial [4], anti-inflammatory [5] and pro-angiogenic [3]. The life-span of MSC in culture is limited. Nevertheless, high numbers of MSC are required for *in vitro* studies and for *in vivo* applications; therefore increasing their proliferative capacity *in vitro* would have important implications for both basic and translational research [6].

Multiple strategies have been devised to increase the life-span of normal human cells in culture. Immortalization and cell reprogramming are commonly achieved via the insertion of various regulative sequences in the genome of the target cells. Such manipulations bring the risk of insertional mutagenesis along with modifying the initial properties of the cells [7]. As an alternative, the use of antioxidants [8], conditioned extracellular matrix [9] and human embryonic stem cell (hESC)-conditioned medium obtained in hypoxic conditions [10,11] have been used to expand the proliferative capacity of primary MSCs.

Here, we used the unconditioned or hESC-conditioned mTeSR1 medium in combination with Matrigel® or hESC-conditioned extracellular matrix (EM) to enhance the proliferative properties of previously described IPI-SA3-C4 primary preadipocyte cells [12]. We found that 1:1 mix of L15 and mTeSR1 ("L15-mTeSR1") increased the proliferative capacity of IPI-SA3-C4 cells by 13 population doublings (PD) while preserving their adipogenic capacity. Furthermore, we found that increased expression of *hTERT* was specifically correlated with increased proliferative capacity and its inhibition led to the dramatic decrease in cell proliferation.

2. Methods

2.1. Culture of IPI-SA3-C4 cells

IPI-SA3-C4 cells (initially 46 PD) were cultured on uncoated or Matrigel®-coated dishes; or on extracellular matrix conditioned by hESC. For this the hESC line H9 was cultured for 4 days and cells were removed using 0.5 M EDTA. Standard culture medium: L15-Leibovitz (Sigma) supplemented with 10% of fetal bovine serum (HyClone) and penicillin 80 U/mL and streptomycin 80 μg/mL (L15). The hESC-conditioned medium was harvested the same day of the culture medium change and diluted in L15.

For short-term growth assays cells were seeded at 5.3×10^3 cells/cm^2 and counted every 24 or 48 h for 6 or 14 days. Doubling time T(d) = 48h/log2 (N_2/N_1), (N_1. initial cell count; N_2 - cell count after 48 h) [13].

For long-term growth assay the cells were seeded at 3.4×10^3 cells/cm^2. Every 3 days the cells were harvested, counted, and reseeded at initial cell density. Population doubling number (PD) (n/(n-1)) = log (Nn/Nn-1)/log2, (n – passage number; N - number of cells) [14].

For colony-forming assay 100 IPI-SA3-C4 cells were seeded per 60 mm diameter culture vessel. After 15 days the vessels were fixed in 3.7% formalde-

* Corresponding author. Institute of Molecular and Cell Biology, University of Tartu, Riia 23b, Tartu 51010, Estonia.
E-mail address: viljar.jaks@ut.ee (V. Jaks)